

# Predicting fleet-vehicle energy consumption with trip segmentation

by

Autumn Umanetz

B.A.Sc, University of Waterloo, 1995

A Thesis Submitted in Partial Fulfillment  
of the Requirements for the Degree of  
Master of Applied Science  
in the Department of Mechanical Engineering

©Autumn Umanetz, 2021

University of Victoria

All rights reserved. This thesis may not be reproduced in whole or in part, by photocopy or other means, without the permission of the author.

Predicting fleet-vehicle energy consumption  
with trip segmentation

by

Autumn Umanetz

B.A.Sc, University of Waterloo, 1995

Supervisory Committee

Dr. Curran Crawford, Co-Supervisor

Department of Mechanical Engineering

Dr. Nedjib Djilali, Co-Supervisor

Department of Mechanical Engineering

# Abstract

This study proposes a data-driven model for prediction of the energy consumption of fleet vehicles in various missions, by characterization as the linear combination of a small set of exemplar travel segments.

The model was constructed with reference to a heterogenous study group of 29 light municipal fleet vehicles, each performing a single mission, and each equipped with a commercial OBD2/GPS logger. The logger data was cleaned and segmented into 3-minute periods, each with 10 derived kinetic features and a power feature. These segments were used to define three essential model components as follows:

- The segments were clustered into six exemplar travel types (called "eigentrips" for brevity)
- Each vehicle was defined by a vector of its average power in each eigentrip
- Each mission was defined by a vector of annual seconds spent in each eigentrip

10% of the eigentrip-labelled segments were selected into a training corpus (representing historical observations), with the remainder held back for testing (representing future operations to be predicted). A Light Gradient Boost Machine (LGBM) classifier was trained to predict the eigentrip labels with sole reference to the kinetic features, i.e., excluding the power observation. The classifier was applied to the held-back test data, and the vehicle's characteristic power values applied, resulting in an energy consumption prediction for each test segment.

The predictions were then summed for each whole-study mission profile, and compared to the logger-derived estimate of actual energy consumption, exhibiting a mean absolute error of 9.4%. To show the technique's predictive value, this was compared to prediction with published L/100km figures, which had an error of 22%. To show the level of avoidable error, it was compared with an LGBM direct regression model (distinct from the LGBM classifier) which reduced prediction error to 3.7%.

# Contents

<b>Front Matter</b>	<b>i</b>	4.3 Classification Algorithm . . .	42
Title Page . . . . .	i	4.4 Classification Method . . . . .	48
Supervisory Committee . . . . .	ii	4.5 Energy Prediction . . . . .	49
Abstract . . . . .	iii	4.6 Parameter Refinement . . . . .	50
Contents . . . . .	iv	4.7 Comparison Predictions . . . . .	55
List of Figures . . . . .	v	<b>5 Results</b>	<b>57</b>
List of Tables . . . . .	vi	5.1 Presentation of Error . . . . .	58
Glossary . . . . .	vii	5.2 Discussion . . . . .	60
Acknowledgements . . . . .	viii	5.3 Application . . . . .	65
<b>1 Introduction</b>	<b>1</b>	5.4 Shapley Additive Explanation	68
1.1 Overview . . . . .	1	<b>6 Conclusions</b>	<b>71</b>
1.2 Project Context . . . . .	4	<b>7 Recommendations and Future Work</b>	<b>73</b>
1.3 Research Structure . . . . .	8	7.1 Assumptions . . . . .	73
<b>2 Background</b>	<b>12</b>	7.2 Cleaning Decisions . . . . .	76
2.1 Travel Data . . . . .	12	7.3 Data Structure . . . . .	78
2.2 Machine Learning . . . . .	16	7.4 Modeling . . . . .	81
2.3 Data Collection . . . . .	23	7.5 Data and Features . . . . .	83
<b>3 Data Cleaning and Preparation</b>	<b>27</b>	7.6 Applications . . . . .	86
3.1 Raw Data . . . . .	27	<b>8 Bibliography</b>	<b>88</b>
3.2 Speed Data Cleaning . . . . .	30	<b>A Logger features</b>	<b>100</b>
3.3 Power Data Cleaning . . . . .	32	<b>B Embodied energy and Fuel Intensity</b>	<b>101</b>
3.4 Regularization . . . . .	35		
<b>4 Methodology</b>	<b>37</b>		
4.1 Feature Preparation . . . . .	37		
4.2 Clustering . . . . .	41		

# List of Figures

- 1 Decision support data-flow and work-flow . . . . . 10
- 2 UDDS and HWFET drive cycles . . . . . 13
- 3 Sample counts by vehicle, studied and non-studied . . . . . 28
- 4 Data collection timespans for individual vehicles . . . . . 29
- 5 Trip SOC vs Voltage . . . . . 34
- 6 SOC and V vs time . . . . . 34
- 7 Linear interpolation problems . . . . . 36
- 8 Timeseries trace of speed and accelerations, overlaid with eigentrip labels . . . . 38
- 9 Feature value distributions, including end-of-range values . . . . . 40
- 10 Feature value distributions after removing common end-of-range values . . . . . 40
- 11 Clustering example vehicle . . . . . 43
- 12 Example of a single-node decision tree, or "stump" . . . . . 45
- 13 MAPE surface vs K and PS (broad) . . . . . 50
- 14 MAPE surface vs K and PS (narrow) . . . . . 51
- 15 Prediction and classification error vs K and PS . . . . . 52
- 16 Final clustering (K=6 PS=7), PCA kinetic features, and power . . . . . 53
- 17 Power by vehicle category and eigentrip . . . . . 54
- 18 Segment prediction error distribution . . . . . 61
- 19 Example power vs prediction . . . . . 62
- 20 Feature value distribution by eigentrip . . . . . 64
- 21 SHAP explanation summaries . . . . . 69

# List of Tables

1	Vehicle LCA . . . . .	6
2	Kinetic features for study . . . . .	15
3	Derived ICE features . . . . .	16
4	OBD2 Log Problem Example . . . . .	24
5	Data Collection Statistics . . . . .	28
6	Speed data cleaning impact . . . . .	31
7	EV cleaning impact . . . . .	35
8	PCA components for visualization . . . . .	44
9	LGBM hyperparameters selected for optimization . . . . .	51
10	Error by timescales . . . . .	60
11	Trip error by vehicle categories . . . . .	60
12	Mission error by vehicle categories . . . . .	66
13	SHAP single prediction . . . . .	68
14	CRD FleetCarma logger features . . . . .	100
15	Vehicle LCA calculations 2018 . . . . .	102
16	Vehicle LCA calculations 2030 . . . . .	102

# Glossary

<b>BAU</b>	business-as-usual	<b>MAPE</b>	mean absolute percentage error
<b>BEV</b>	battery electric vehicle	<b>MMAPE</b>	modified mean absolute percentage error
<b>CAN</b>	controller area network	<b>mission</b>	typical whole-study travel pattern observations for a specific vehicle
<b>CRD</b>	Victoria Capital Regional District	<b>ML</b>	machine learning
<b>CSV</b>	comma-separated-value	<b>MOE</b>	Canadian Ministry of Environment & Climate Change Strategy
<b>ECU</b>	engine control unit	<b>MSE</b>	mean-square error
<b>EM</b>	expectation maximization	<b>OBD2</b>	on-board diagnostic system v2
<b>EV</b>	electric vehicle	<b>PCA</b>	principle component analysis
<b>FCEV</b>	hydrogen fuel-cell electric vehicle	<b>PID</b>	parameter identifier
<b>GHG</b>	greenhouse gas	<b>PAE</b>	percent absolute error
<b>GMM</b>	Gaussian mixture model	<b>PHEV</b>	plug-in hybrid electric vehicle
<b>GPS</b>	global positioning system	<b>PS</b>	power-scaling factor
<b>GWP</b>	global warming potential	<b>Q95</b>	95th percentile
<b>HEV</b>	hybrid electric vehicle	<b>Q98</b>	98th percentile
<b>HV</b>	high-voltage	<b>RPM</b>	revolutions per minute
<b>HWFET</b>	highway fuel economy test	<b>SAE</b>	Society of Automotive Engineers
<b>ICEV</b>	internal combustion engine vehicle	<b>SHAP</b>	Shapley additive explanations
<b>ICE</b>	internal combustion engine	<b>SOC</b>	state of charge
<b>IQR</b>	inter-quartile range	<b>SSE</b>	sum of squared errors
<b>K</b>	number of clusters in K-means clustering	<b>UDDS</b>	urban dynamometer driving schedule
$L_e$	equivalent to litres of gasoline	<b>US EPA</b>	United States Environmental Protection Agency
<b>LCA</b>	life-cycle analysis	<b>ZEFI</b>	Zero Emissions Fleet Initiative
<b>LGBM</b>	light gradient boosting machine		
<b>LVQ</b>	learning vector quantization		
<b>MAF</b>	mass-airflow		

# Acknowledgements

In writing this thesis, I have benefited from many kinds of assistance from a remarkable assortment of people at the Victoria Capital Region District (the CRD), the University of Victoria's Institute for Integrated Energy Systems (IESVic), and the Sustainable Systems Design Lab (SSDL).

My work could not have been conducted without the CRD's commitment to sustainability and green transportation. The CRD's generous funding and donation of logger data has been the cornerstone of this research, and I am very grateful for the opportunity to participate in the Zero-Emission Fleet Initiative (ZEFI) and the Smart Fleet project. In particular I'd like to single out Liz Ferris, Maryanna Kenney, and Dave Goddard for their enthusiastic advice on practically bringing sustainability to fleet operations.

My supervisors, Dr. Curran Crawford and Dr. Ned Djilali have been excellent advisors, and enthusiastic providers of advice, instruction, and encouragement. I have deeply appreciated the opportunity to work closely with them.

I've also benefited greatly from my association with Dr. Stephen Neville, who taught me the skills to perform robust large-scale analysis, and Dr. Ted Darcie, who has helped me many times to find appropriate middle ground between perfect and possible.

My colleagues in the Sustainable Systems Design Lab have created a welcoming community out of a diverse range of backgrounds and interests, and I've felt privileged to be part of it. In particular, I'd like to thank Markus and Rad for making it into a community, and my labmates Julian, Orhan, Charlotte, Marvin, and Graham for creating a great place to work.

The deepest thanks of all go to my thesis-widow and partner in everything, Sarah, whose turn it is now.

# 1 Introduction

1.1	Overview . . . . .	1	1.2.3	Simple distance-based fuel consumption . . . . .	6	
	1.1.1	Problem statement . . . . .	1	1.3	Research Structure . . . . .	8
	1.1.2	Goals and motivations . . . . .	1	1.3.1	Research hypothesis . . . . .	8
	1.1.3	Document outline . . . . .	3	1.3.2	Model validity and predictive power . . . . .	9
1.2	Project Context . . . . .	4	1.3.3	Preliminary validation . . . . .	9	
	1.2.1	CRD ZEFI project . . . . .	4	1.3.4	Research contributions . . . . .	9
	1.2.2	Operational and embodied emissions . . . . .	4			

## 1.1 Overview

### 1.1.1 Problem statement

In the effort to reduce operational fleet greenhouse gas (GHG) emissions, one important tool is the selective replacement of individual vehicles with low-emission alternatives. Given limited capital, it is important to ensure that the correct vehicles are targeted for replacement in the course of rightsizing, ongoing fleet turnover, or policy-driven phased replacement of individual high-emission vehicles.

No clear path is seen to directly modelling the GHG emissions of existing and replacement vehicles. However, a change in operational CO2 emissions can be inferred with reasonable accuracy from the change in the quantity and type of fuel consumed. It should be possible to predict the change in GHG footprint by modelling the change in operational energy consumption caused by vehicle replacement, and applying an appropriate fuel-specific emission intensity factor.

### 1.1.2 Goals and motivations

Fleet vehicles are typically assigned to perform an ongoing specific set of duties, commonly referred to as a "mission." In order to more easily predict GHG emission changes resulting from mission-vehicle replacement, this thesis proposes a data-driven model for

estimating the change in input energy consumption associated with assigning new vehicles to existing, well-known roles.

In other words, the model will be suitable for estimating the GHG emissions reduction associated with performing a known mission profile with a different vehicle. As discussed below in §1.2.2, this approach is specific to operational emissions, a decision which is limiting, but appropriate for use with many current policy initiatives, such as the municipal GHG action plan [1] that inspired this work.

Since one important application is in a decision support tool for non-technical fleet managers, it should be accessible to the end-user without installing custom software. Even a cloud-hosted service may violate privacy requirements – the movements of individual vehicles are considered protected private information by many organizations.

The traditional method of predicting vehicle operational energy consumption – applying distance-based L/100km fuel economy ratings such as those provided by Natural Resources Canada [2] or the US EPA [3] – is held to be too inaccurate for travel which does not precisely match the conditions under which the ratings were measured [4, 5].

Conversely, a fully accurate fuel consumption model that infers nonlinear relationships from a much larger list of operational properties would have impractical data collection requirements, and would require the distribution and management of specialized software. The source data may provide information regarding the movements of fleet users, and there would be significant privacy and security concerns if a model were to be cloud-deployed [6]. These criteria would make such a model impractical for use as a fleet procurement decision support tool. Such a model would potentially be so computationally expensive that the model itself would have a significant GHG footprint.

In short, in order to promote emissions reduction, it is desirable to develop a new method for predicting operational vehicle energy consumption in fleets, which is:

- simple enough to perform in a spreadsheet
- does not require massive cloud computing overhead
- requires a minimum amount of data collection

- is more accurate than distance-based economy ratings

This thesis explores the development of a data-driven model that will meet all of these criteria, in the context of vehicles with logger data, and mission profiles which have been previously logged.

### 1.1.3 Document outline

This document begins with an extensive **Introduction**, which (a) lays out the above overview of the problem, motivation and goals, (b) describes the research context in terms of municipal partnership that provided the data and informed the motivations, and (c) explains the structure of the research problem.

The remainder of the document roughly follows the chronology of the research effort, as follows:

§2. The **Background** section provides a literature review, and a summary of background material fundamental to understanding the topic and approach.

§3. **Data Cleaning and Preparation** was a key and challenging element of the work undertaken, and was sufficiently involved to merit its own section.

§4. The actual machine learning techniques used to build the predictive model are described in **Methodology**.

§5. The model's predictive error is evaluated, its value is demonstrated by comparison with  $L_e/100\text{km}$ , and avoidable error quantified by comparison to an ML regression model in **Results**.

§6. Finally, the findings are wrapped up and summarized in the form of a short section of **Conclusions**.

§7. Lays out a number of potential topics for further refinement, exploration and other **Recommendations and Future Work**.

## 1.2 Project Context

### 1.2.1 CRD ZEFI project

As a part of the Victoria Capital Regional District (CRD)'s Zero Emissions Fleet Initiative (ZEFI) project, a number of vehicles in the CRD fleet were equipped with FleetCarma on-board diagnostic system v2 (OBD2) telematic logging devices at various periods for approximately a year starting in early 2018 [7].

A motivating goal in this project was to determine actions needed to meet the organization's GHG reduction targets, given that 47% of the CRD's baseline 2007 GHG emissions resulted from fleet fuel consumption [1]. An early finding was that, at least on the restricted basis of range requirements, nearly all of the studied vehicle missions could be executed by current battery electric vehicles (BEVs) [8].

Further detail on the nature of the data collection and the logged data is presented in §2.3.1.

### 1.2.2 Operational and embodied emissions

The intent of this research is to address a core accessibility problem for modelling fleet operational emissions, as needed to address reduction goals similar to those of the CRD's ZEFI program.

For internal combustion engine vehicles (ICEVs), this reduces to tailpipe emissions, calculated by estimating the fuel directly consumed by the vehicle – traditionally called "tank-to-wheel" energy. For gasoline, the GHG emissions of this energy are estimated at an intensity of  $88.1 \text{ g CO}_2\text{/MJ}$  [9]. For electric vehicles (EVs), this is a reflection of the emissions associated with the grid electricity consumed by the drive motor, at the utility's published carbon intensity. For BC Hydro, this is  $10.67 \text{ t CO}_2\text{/GWh}$  [10] ( $2.96 \text{ g CO}_2\text{/MJ}$ ).

The BC GHG Reduction Act [11] references the 2007 baseline GHG inventory report [12] as a baseline. Emissions in the inventory report are attributed to the jurisdiction

where emission is *generated*, rather than the jurisdiction where the *benefit* of the emission accrues. E.g. if H<sub>2</sub> gas or lithium-ion batteries are used in BC, the associated manufacturing emissions are attributed to the foreign H<sub>2</sub> steam reformation plant or battery factory, rather than to the BC point of beneficial use. This may be seen as constituting a perverse incentive, insulating end-users from any financial costs associated the embodied emissions of manufactured goods, and driving manufacturing to under-regulated jurisdictions.

In the late 2010s there were claims in the US popular press such as [13, 14] that BEVs have a higher lifetime GHG impact than equivalent ICEVs. Anecdotally, the claims are sometimes echoed by concerned Canadian citizens. The core argument appears to be that BEV proponents ignore or under-represent emissions associated with manufacturing the battery pack, and the high carbon intensity of some sources of grid electricity. Although this probably constitutes an example of the "balance-as-bias" fallacy [15], a short discussion is warranted regarding the full cradle-to-grave lifecycle analysis for different light vehicle technologies and their fuel sources.

A 2018 comprehensive comparison by Elgowainy et al [16] summarized full cradle-to-grave GHG emissions (including fuel cycle and manufacturing cycle), for several different types of light vehicles. The study included ICEVs, hybrid electric vehicles (HEVs), plug-in hybrid electric vehicles (PHEVs), hydrogen fuel-cell electric vehicles (FCEVs) and BEVs, as well as other vehicle types excluded from this discussion. Retaining that study's figures for manufacturing and fuel efficiency, but applying current and forecasted 2030 intensities for the appropriate fuel pathways for BC as follows, it is clear that alternative fuel vehicles have a significant and improving advantage, shown in table 1. Some discussion of the assumptions and calculations for this comparison appears in appendix B.

Ultimately, the scope of this research is constrained to local tailpipe emissions as required for the planning requirements of organizations like the CRD. It explicitly excludes a full carbon lifecycle analysis, including all carbon emissions embodied in the vehicle's manufacture and eventual recycling, as well as all carbon emitted or embodied

Table 1: Current and 2030 vehicle combined operational and embodied LCA GHG footprint, at BC fuel carbon intensities

Vehicle	2018		2030	
	Fuel Intensity (g CO <sub>2</sub> e/MJ)	Emissions (g CO <sub>2</sub> e/km)	Fuel Intensity (g CO <sub>2</sub> e/MJ)	Emissions (g CO <sub>2</sub> e/km)
ICEV	88.1	295	70.5	187
HEV	88.1	221	70.5	130
PHEV35	64.9	129	51.1	83.1
FCEV	5.	48.2	1.18	34.5
BEV90	2.5	29.6	1.11	23.1

by associated infrastructure for manufacture, repair, fuelling, and eventual recycling.

### 1.2.3 Simple distance-based fuel consumption

In Canada, light passenger vehicles are labelled with EnerGuide fuel consumption ratings, reflecting their expected performance in typical conditions [17]. This program is similar to the US EPA’s fuel economy database, fueleconomy.gov [18]. The EPA’s fuel economy ratings have been found to be quite inaccurate, with recent studies finding that they predict consumption ranging from 15.5% too low [4] to 17% too high [5] relative to real-world consumption.

EnerGuide numbers result from manufacturer tests of vehicles against defined drive cycles [19], in order to provide an apples-to-apples comparison between vehicles. Prior to 2015, the test platform was a 2-cycle city/highway test (essentially a modified UDDS/HWFET [20]). In 2015, three additional cycles were added, resulting in a 5-cycle test (adding tests to reflect the impacts of cold-weather conditions, aggressive driving, and air conditioning [21]), with incremental updates in 2016 and 2017 [22]. For accessibility, this rating is expressed in units of litres of fuel consumed per 100km driven: L/100km. Non-internal combustion engine (ICE) vehicles are rated in litres-equivalent ( $L_e$ ), at a standard conversion rate of 8.9 kWh per litre of gasoline [23]. Notwithstanding the 2015 change from two to five cycles, three separate fuel consumption numbers are published to reflect city, highway, and combined performance.

This method of predicting consumption is an important baseline, since the fundamental

metric for evaluating an individual vehicle replacement will be "avoided emissions", which quantifies the change in operational emissions associated with replacing a current (incumbent) vehicle, with a lower-emission alternative (replacement) vehicle.

The traditional method of computing avoided emissions is to apply the difference in fuel consumption ratings and fuel carbon intensities between the incumbent (1) vs replacement (2) vehicles, thus:

$$\Delta Emissions = CO_2e^{(2)} - CO_2e^{(1)} \quad (1)$$

$$\text{where } \begin{cases} CO_2e \approx D \times [\eta \times e \times I]^{(vehicle)} \\ D = \text{Distance } (km) \\ \eta_{c/h} = \text{Vehicle's static tested city/hwy fuel economy } (L_e/100km) \\ e = \text{Fuel energy density } (kWh/L) \\ I = \text{CO}_2 \text{ intensity of vehicle's fuel } (kg/kWh) \end{cases} \quad (2)$$

In other words, each vehicle has a pair of characteristic CO2 emission values per km of operation, directly related to its standardized rates of fuel consumption.

This approach is an oversimplification, assuming constant values for  $\eta$ , and neglecting the facts that drivetrains are optimized for specific drive cycles, and that efficiency is impacted significantly by the nature of the driving undertaken. For example: electric-drivetrain vehicles have technologies such as regenerative braking and automatic shutoff, allowing them to perform efficiently in conditions where conventional internal combustion engine (ICE) vehicles are wasteful, such as stop-and-go traffic, or conditions requiring extensive idling. Conversely, a conventional diesel ICE drivetrain is designed specifically to optimize efficiency at constant highway speed, while a series-hybrid in the same conditions would suffer from avoidable energy conversion losses.

## 1.3 Research Structure

### 1.3.1 Research hypothesis

This study proposes and tests the hypothesis that energy consumption for arbitrary periods of vehicle travel can be accurately predicted by decomposing the proposed travel period into a linear combination of characteristic trip segments, each with a known constant characteristic power consumption for each vehicle type. The prediction will be the sum of vehicle-specific energy consumption totals for that combination of segments. The prediction should hold for travel periods ranging in duration from a single trip to a multi-month mission profile.

To simplify further discussion, the following terms are defined:

“*Mission profile*” refers to the operations typically undertaken by a specific vehicle. Municipal examples include "bylaw supervisor", "meter reader", and pool vehicle".

“*Kinetic travel data*” refers to a specific portion of a vehicle’s speed history, or summary statistics derived from it.

“*Eigentrips*” are a basis set of vehicle-agnostic travel segments with the following characteristics:

- Each eigentrip is defined by characteristic kinetic travel data
- Every vehicle has characteristic energy consumption for each eigentrip
- All historical and predicted travel data can be decomposed into a linear combination of eigentrips

The primary technical problems addressed in this thesis are:

- Selecting an appropriate basis set of eigentrips using kinetic travel data.
- Evaluating the predictive power of a linear combination of eigentrips, relative to the observed energy consumption of vehicles on specific missions.

### 1.3.2 Model validity and predictive power

The new method's validity will be evaluated by comparing its prediction error to the real-world energy consumption, as inferred from the full raw dataset. This prediction error will be contrasted with the prediction error of the traditional distance-based fuel economy statistic described above in §1.2.3.

It is worth noting that the "observed energy consumption" baseline is an estimate of unknown accuracy derived from the available proxy values (MAF and SOC) as discussed in §3.3. This assumption is addressed in §7.5.2.

### 1.3.3 Preliminary validation

The author conducted a preliminary experiment [24] as a coursework project, studying 300 hours of kinetic travel data and fuel flow rates inferred from MAF (mass-airflow) values, for ten similar vehicles.

In that study, the data was partitioned into 10-minute segments by clock time (segment boundaries were placed at even 10-minute intervals starting at the top of each hour). A fingerprint of representative statistics was then calculated for each segment. K-means clustering [25, §10.4.3] was performed on the resultant dataset to find three clusters. Based on the clustering results, held back test data was classified with a softmax [25, §6.6.2] logistic classifier [26], and engine load was predicted. The average engine load prediction error using this method was approximately 2%.

Although not proven to generalize, the result was sufficient to suggest that the method warranted further study.

### 1.3.4 Research contributions

This research explores and validates a new method for predicting the energy consumption of different vehicle types when used to execute a well-known mission profile.

The method requires logger data attainable with nearly any commodity OBD2 logger – although some care must be taken to assure the quality of fuel / energy consumption

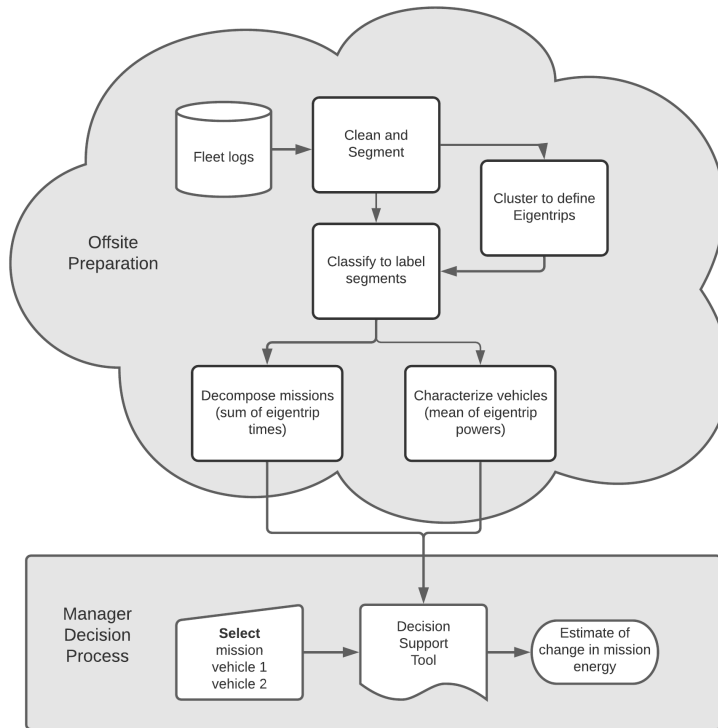


Figure 1: Decision support data-flow and work-flow

data. The data will be used to calculate characteristic parameters describing the study vehicles and mission profiles. The characteristic parameters can then be used to predict energy consumption according to a simple linear calculation that can be implemented in a spreadsheet-based decision support tool. A potential data-flow is shown in figure 1, illustrating the path that the data takes from initial capture, through the generation of the decision-support spreadsheet. This figure also illustrates the fleet manager's workflow, where a known mission is selected from those listed in the tool, along with a pair of vehicles (presumably the incumbent and a potential replacement), resulting in a predicted change in energy footprint.

This will allow fleet managers to accurately predict the energy requirements (and hence GHG emission footprint) of any logger-equipped vehicle, applied to any mission profile which has been previously performed by any other logger-equipped vehicle. In other words, the characterization of the fleet's various *missions* can be collected by any ICEV or BEV. The collection of logger data to compute characteristic energy consumption for the same or other vehicles of the same type can be collected on entirely different

routes/missions, and even by entirely different organizations. Sharing real-world vehicle performance data between organizations would improve estimation of energy consumption based on different procurement scenarios, including new vehicle models of which a given organization has no direct experience – in much the same manner as  $L_e/100km$  figures are currently used.

Other research contributions include:

- Shapley additive explanations (SHAP) showing the relative importance of various input features to the prediction of input power.
- a technique for reconstructing serial OBD2 values that have been tabularized
- evaluation of error inherent in traditional L/100km technique
- comparison to direct regression, to gauge efficacy & accuracy of both proposed method and L/100km method

## 2 Background

2.1	Travel Data . . . . .	12	2.2.5	Clustering . . . . .	20	
	2.1.1	Drive cycles . . . . .	12	2.2.6	Classification . . . . .	22
	2.1.2	Microtrips . . . . .	14	2.2.7	Gradient boost and LGBM	23
2.2	Machine Learning . . . . .	16	2.3	Data Collection . . . . .	23	
	2.2.1	Feature selection . . . . .	16	2.3.1	OBD2 logger implementa-	23
	2.2.2	Time-series analysis . . . . .	18		tion . . . . .	
	2.2.3	Binning and segmentation . . . . .	19	2.3.2	Fuel vs airflow . . . . .	25
	2.2.4	Regression analysis . . . . .	19			

This section addresses background material fundamental to the topic. Quantitative analysis of travel patterns is typically performed on data comprising *drive cycles* and *microtrips*, so a brief background on these concepts is presented.

The proposed method involves *feature selection, clustering, and classification* of multi-dimensional timeseries data, so various tools for these tasks are discussed.

Finally, this section contains a short background of the technology used for *data collection*, and limitations around the collection of *fuel flow rates*.

### 2.1 Travel Data

#### 2.1.1 Drive cycles

A drive cycle (or driving cycle) is the speed-time data that describe a portion of a vehicle’s travel history [27], either measured, generated, or synthesized. A large number of standardized drive cycles have been published by various government agencies and private organizations, to facilitate optimization and testing to standardized benchmarks [28].

Two of the most heavily-referenced examples are the urban dynamometer driving schedule (UDDS) and highway fuel economy test (HWFET) cycles [29], defined by the United States Environmental Protection Agency (US EPA), and shown in figure 2. Elevation

and grade are not a fundamental part of the generally accepted drive cycle definition and no mention is made of these in UDDS, HWFET, nor the other drive cycles referenced in the EPA’s federal test procedure [1]. However, vehicle performance is strongly impacted by road grade, so an elevation profile is often used in parallel for simulations [30]. As discussed in §7.5.3, the road grade information used in this study was not of particularly high quality, and the topic merits additional work.

In machine learning, "classification" is the process of labelling an observation with a discrete nominal label (e.g., a category name) which best corresponds, on the basis of a set of "training" observations with known labels [25]. Drive cycle classification has been the subject of a substantial body of work. A frequent topic is the optimization of HEV battery energy management, such as the work of Wu et al on fuzzy energy management [31], with the goal of determining whether a vehicle was being operated in urban, suburban, or highway conditions. This paper used fixed-length partitions of 3 minutes, to match the typical urban stop-go-stop cycle length.

Other papers had goals such as BEV range estimation by Yu et al [32], or optimization for battery size (Redelbach et al) [33] and battery lifespan (Smith et al) [34].

However, most treatments of the subject do not restrict themselves to easily-logged kinetic parameters, but include classification features such as engine power, road gradient, and road-type. Indeed, in many papers, the data was collected by shadowing each subject vehicle with a chase-car, a method that is prohibitive for any kind of fleet data collection at scale.

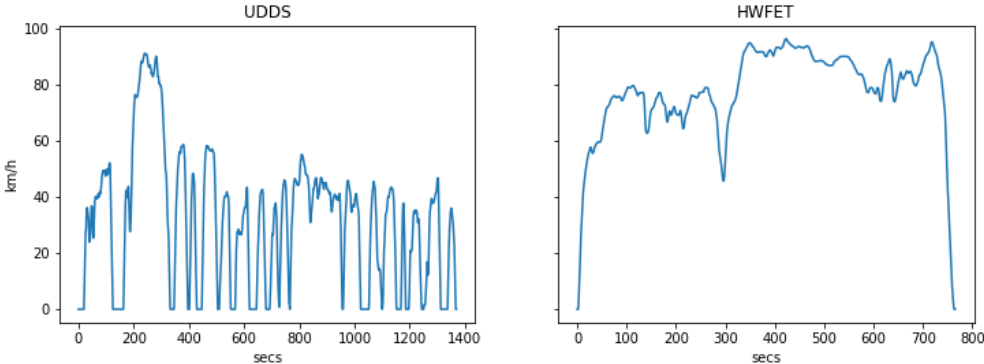


Figure 2: UDDS and HWFET drive cycles

### 2.1.2 Microtrips

Microtrips are "the sections of travel between consecutive stops", first used for travel analysis by General Motors Research in 1976 [35], where it was used to demonstrate that fuel rate varied linearly with average trip speed (true of the automotive technology of the time). They are used frequently as an aid to the development of new drive cycles, as per Kamble et al [36], where synthetic geography-specific drive cycles were created from a number of real microtrips.

The microtrip concept has seen very little use in the problem of drive cycle classification, with only a couple of examples seen in the literature. One example is described by Shankar and Marco in [37], which applies neural network classification to determine the road-type (e.g., highway, arterial, or local), as well as a congestion index, for use in predicting an input power appropriate to the driving conditions. However, the method was addressed specifically to battery vehicles, and presumes that the only factors influencing energy consumption are derived from road congestion and type. The method does not consider the possibility that different travel types in the same context might have different energy requirements, for example because the mission requires regular stops or extensive idling.

Shankar and Marco's paper does point out an inherent limitation of microtrips: that they are defined from stop to stop. This means that a single microtrip is likely to encompass more than one type of travel, and/or to unnecessarily segment a single type of travel that includes stops.

Another relevant example [38] by He et al extracted microtrips from the definitions of several predefined drive cycles, calculated the first seven of the aggregated velocity-derived features shown in table 2, and applied principle component analysis (PCA) to retain four principal components. These principal components were calculated on segments of actual travel data, in order to classify the segments in an learning vector quantization (LVQ) neural net, with very good classification results. The first seven features gave excellent classification results and may be expected to provide an excellent

Table 2: Studied kinetic features, as derived from logger data

Description	Units
Mean speed	( $km/h$ )
Max speed	( $km/h$ )
Mean acceleration	( $m/2^2$ )
Max acceleration	( $m/s^2$ )
Mean deceleration	( $-m/s^2$ )
Max deceleration	( $-m/s^2$ )
Idle time fraction	(%)
Mean climb	( $m/s$ )
Mean descent	( $m/s$ )
Acceleration reversals	( $\#/s$ )
Power	( $kW$ )

starting point for fuel consumption prediction. However, features were excluded from that work, which will contribute to fuel consumption in a heterogeneous fleet; road grade and a count of acceleration reversals were added, and other non-studied examples include payload, accessory load, and others discussed in §7.5.

He’s technique is not directly applicable to fleet fuel prediction, for a number of reasons:

- The technique was only demonstrated on artificial drive-cycles, and may not perform well on the complexity of real local driving conditions
- The exemplar microtrips are not shown to be predictive of fuel consumption between vehicle types
- PCA uses the largest eigenvectors to project data onto the lower-dimensional space that best represents the data’s variation [25]. By design, PCA is an unsupervised technique with no relationship to regression; it captures the variance of the individual input features by weighting them accordingly, but without explicit regard to their relationship to the target variable. Hence, the weight of a feature in the principal components is not indicative of whether it has predictive power.

In general, the body of work on microtrips is informative with regards to feature selection and supports the notion of predictive analysis by decomposition. However, the fundamental definition of a micro-trip as a “stop-go-stop” cycle means that it is likely to mix some types of travel that should be separated, and to artificially partition others

Table 3: Derived ICE features with relative impact on fuel consumption [39]

Relative impact	Factor description
5	stop
4	acceleration with strong power demand
2	speed oscillation
2	acceleration with moderate power demand
2	extreme acceleration
-2	speed 50+/-70
-2	moderate engine speeds at gears 2 and 3
1	late gear changing from gear 2 and 3
-1	deceleration
-1	speed 70+/-90
-1	low engine speed at gear 4
-1	low engine speed at gear 5
0	speed 15+/-30
0	speed 90+/-110
0	engine speed > 3500
0	speed > 110

that would more effectively be considered as a unit.

## 2.2 Machine Learning

### 2.2.1 Feature selection

In machine learning, a “feature” is a measured property of the system under study, and usually implies a dimension in the system’s state-space, either direct or a projection. It is not always obvious which features are salient for a given problem, so careful consideration of the problem is required with respect to the available data, plus experimentation, pre-processing, and investigation. There are a number of important problems that can arise from an improper choice of features for use in a machine-learning model.

When aspects of a feature’s behaviour can be probabilistically predicted from knowledge of another feature (such as when the features are correlated, or otherwise functionally related), the two features are said to share “mutual information” [25, §A.7.3]. For most cost or distance functions, error related to given information is redundantly counted for every additional feature axis on which the information is represented. In many machine

learning algorithms, this has potential to create a problem wherein the learning system over-values the importance of the duplicated information.

The curse of dimensionality [40] refers to the counter-intuitive fact that adding additional features will degrade accuracy for many forms of machine learning. This property devolves out of two geometric properties of high dimensional spaces.

First, the state-space volume expands exponentially with the addition of dimensions, quickly leading to a sample density too low for generalizable classification. A second property, called the “concentration of norms,” refers to the surface area of a hypersphere expanding faster than its volume with the addition of dimensions – meaning that in a set of data normally distributed in multiple dimensions, most points will lie in the tail of at least one dimension. In this situation, it is easy to inadvertently construct an arbitrary classifier which works extremely well on the existing data, but which does not generalize – a situation referred to as over-fitting [41]. Together, these issues mean that intuition is not informative as to the behaviour of high-dimensional models, and the feature set should be minimized as much as practical.

The question of which loggable features are most clearly related to fuel consumption and/or emissions was addressed comprehensively for conventional ICE vehicles in [39]. In this study, 62 logged and derived features were investigated, and reduced to the most important compound features using PCA and factor analysis (which is similar to PCA in that it attempts to find a lower-dimensional representation, but dissimilar in that it accounts for correlations among the features [25]). These techniques are problematic in that PCA selects for high variance but not prediction, and factor analysis corrects for correlation, but not for any other forms of mutual information. Nevertheless, the resultant set of factors seems to be an excellent starting point for selecting features that will describe the fuel consumption rate of ICE vehicles. The relative impact on fuel consumption (in units of 1/10ths of a standard deviation) of several of the compound factors found in Ericsson’s study are shown in table 3.

### 2.2.2 Time-series analysis

Time-series data consists of sequential measurements of the same feature over time, with the characteristic property that the data are generated by a process, and are not statistically independent of earlier samples in the process [42]. A drive-cycle is an excellent example, describing a trip in terms of measurements of the vehicle’s speed over time.

Time-series data is commonly analyzed by the direct application of time-domain analysis techniques – finding patterns and behaviours with respect to temporal ordering. In the context of trip-segment similarity, it seems intuitively obvious that order does *not* much matter, relative to many other aspects of the driving patterns. For example: the segments of the urban drive cycle, driven in reverse order, could be expected to have energy consumption very similar to that of the forward-ordered version (stipulating a similar net elevation profile), but it is hard to imagine a meaningful time-domain measure that would expose the similarity. This intuition suggests that time-domain analysis techniques will miss important commonalities between trips.

Transforming into the frequency domain can address this problem and give insight into the relative importance of various cyclical behaviours. Applied to segments of kinetic driving data, it might give insight into the rate of start-stop or speed-slow cycles, where they exist. However, since acyclic behaviours might be critical differentiators, and would be lost in the transformation out of the time domain, we certainly cannot rely on frequency analysis alone.

Apart from the inter-sample interval necessary to calculate acceleration, the key features used in this research draw no useful information from their time sequencing. Thus, for the insights to be derived from the data, time series techniques do not provide a great deal of analytical power, and are left as a topic for future investigation (§7.3).

### 2.2.3 Binning and segmentation

Data binning is the process of grouping data points with similar values together, such that they can be referenced by a common value. This is useful to reduce the volume of data for faster processing, or to improve its comprehensibility, as with histograms. Segmentation is conceptually similar; it consists of partitioning time series data into time intervals, allowing each segment to be characterized as a group [43].

A key technique used in this research combines both techniques: partitioning the data into fixed-length segments, which are thereafter treated as non-time series bins. A selection of representative summary statistics (a fingerprint) for each segment are calculated, after which the time information can be discarded or ignored. Similar segments can then be binned, allowing the application of simple and intuitive non-time series analytical techniques.

This has the advantage that the similarity measure between segments can be as simple as Euclidean distance, or as complex as necessary to capture prior understanding of "similarity" for the system in question.

The primary disadvantages of using bin fingerprints are difficulties in (a) determining appropriate statistics such that if two trips are subjectively similar, then their statistics will have objectively similar values, and (b) finding segment boundaries, such that segments do not encompass multiple types.

### 2.2.4 Regression analysis

Regression analysis is a branch of mathematical statistics concerned with quantifying the relationships between some number of variables using statistical data [44]. In the most general sense, this involves finding the appropriate parameters for a mathematical model, which will allow it to calculate predicted values for the dependent variable(s) based on the input values for the independent variables.

The most commonly used example is *linear* regression, which consists of finding the coefficients  $\mathbf{b}$  for the independent variables  $\mathbf{x}$  that will best predict target variable  $y$ ,

typically by minimizing the mean-square error (MSE) for all training values  $\hat{y}$ .

$$y = b_0 + b_1x_1 + \dots + b_nx_n + \epsilon \quad (3)$$

$$MSE = \frac{1}{n} \sum (y - \hat{y})^2 \quad (4)$$

If the relationship between the independent and dependent variables is more complex, nonlinear techniques are used – either by fitting coefficients to a more complex formula that better describes the relationship, or by using some other model entirely, such as a decision tree or artificial neural net [41]. These nonlinear techniques result in a better fit to the observed data, but at the cost of a more complex formula and the risk of overfitting.

Traditional regression techniques are not a good fit for the primary stated goals of this research, as it would not be possible to develop a spreadsheet-deployable model that could clean and process the millions of rows of logger data. Setting aside the unique requirements of a deployable decision support tool, tree or neural net regression would be the simplest path to predicting vehicle energy consumption, and will be used in §5 to provide a basis for comparison of the accuracy of the proposed spreadsheet-capable model.

### 2.2.5 Clustering

Clustering is the general name for unsupervised techniques that have the goal of grouping similar data samples according to an appropriate definition of similarity.

For the problem at hand, it is impractical to manually define a basis set of eigentrips that will (a) adequately represent all travel in the dataset, and (b) be sufficiently discriminatory with regards to fuel consumption between the studied vehicle types. In this study, the entire corpus of segmented travel data will be clustered, and the characteristics of each group will be considered to represent one eigentrip. This section will address appropriate methods for clustering.

The simplest and arguably most intuitive clustering technique is K-means clustering, most easily understood with an interactive visualization, such as the one linked at [45]. The technique consists of selecting a number ( $k$ ) of randomly distributed cluster centroids, assigning every data point to the cluster defined by the nearest centroid, and then iteratively redefining each cluster centroid as the mean of its constituent points. The technique's simplicity is balanced by two significant limitations. First, it must be provided with a predefined cluster count [25], which is a key tuning parameter. Second, it presumes clusters in normal, spherical distributions; its cost function is most appropriate for points which have a Gaussian distribution of equal variance in every dimension.

The technique can be generalized to data in non-spherical distributions by maximizing the probabilistic membership in each cluster – this is called expectation maximization (EM) clustering – or more specifically, Gaussian mixture models (GMMs) if the clusters are normally distributed.

Any clustering technique relies on an appropriate definition of distance between points in the feature space. A common and intuitive choice is the L2 norm – Euclidean distance – applied to appropriately normalized features. This works well, because non-discriminatory features are likely to balance themselves by virtue of being equally distributed between the clusters. However, the measure is sensitive to outliers, and cannot account for desired similarities that can only be described by nonlinear combinations of features.

K-means also requires a number of clusters ( $k$ ) as an input. Typically, this number is found by inspection (the "elbow" method [46]) or by minimizing a loss function such as silhouette score [47]) against different values for  $k$ .

In addition to the advantage of simplicity, K-means has a well-known implementation in the Scikit-learn library. Although it presumes spherical, normalized clusters [48], this requirement is also an advantage, since it allows features to be given relative weights by the simple expedient of linear scaling.

There is an obvious argument against the use of K-means: that the best clusters (for

a domain-specific definition of similarity) may not be normal and spherical. However, the travel data at hand is continuous, and does not *have* distinct clusters. For the immediate goal – selecting "similar" data to train the eigentrip classifier, we can allow the clustering algorithm to define the shape of its clusters. Reviewing the impact of alternate clustering techniques on classifier accuracy will be an excellent topic for future refinement of the model.

### 2.2.6 Classification

Classification is similar to regression analysis, but with a goal of predicting a discrete value, rather than a scalar, commonly used for determining which of a fixed number of categories is the best fit for a particular datum [41].

Classification is a key element of the proposed method: each trip segment will be classified and labelled with its most similar eigentrip. If the thesis is correct, the characteristic power of that eigentrip will be similar to the actual power of the trip segment.

Classification algorithm selection is more art than science, with the "No Free Lunch" theorem demonstrating that there is no model that is best across domains [41]. In general, the researcher must evaluate the characteristics of their data and the requirements of their model, and attempt to find an algorithm that suits both.

In this case, since several of the features have unknown multi-modal distributions, Bayesian algorithms will not be a good fit. Neural nets require computationally intensive training, have non-explainable results, and do not extrapolate outside their training volume. The remaining family of classifiers which seem appropriate are ensemble decision trees. The light gradient boosting machine (LGBM) algorithm is selected for initial review as demonstrating a good balance between training speed and prediction accuracy.

### 2.2.7 Gradient boost and LGBM

Model selection is arguably the most difficult aspect of practical, applied ML. The proposed model has aspects that make it particularly challenging:

- features are multi-modal and do not follow a common distribution
- features may have unknown mutual information
- target feature has no obvious structure
- explanation of feature impact on prediction may be important for future work
- millions of data points

The unknown distribution renders Bayesian methods impractical. The possible shared information duplicated between features and potential requirement for explainability comprise good arguments against artificial neural nets. Finally, due to the need for iterative evaluation over the relatively large dataset discussed below in §4.6, slow-training methods would not be practical. Given these exclusions, an ensemble decision tree method warranted consideration.

Although at risk of running afoul of Maslow’s Hammer [49], the common-sense admonition that practitioners are prone to over-application of familiar tools, the popular LightGBM model meets all of the above criteria, described in more detail in §4.3.

## 2.3 Data Collection

### 2.3.1 OBD2 logger implementation

In order to understand a significant primary data collection issue, the reader will require some background on the technology used for data collection.

The dataset used in this study was collected by FleetCarma Inc., a commercial company based in Waterloo, Ontario. FleetCarma uses telematics loggers connected to the vehicles’ OBD2 interface. OBD2 is a protocol defined by Society of Automotive Engineers (SAE) standard J1962 for vehicle data access, and specifies a female 16-pin electrical connector for access, commonly known as the OBD2 port. It accesses the

vehicle’s controller area network (CAN) bus, a serial hardware layer commonly used to transport vehicle sensor data between various engine control unit (ECU)s. Information in this subsection is summarized primarily from an instructional website [50] and the original Texas Instruments application document [51].

Devices on a CAN bus communicate exclusively by broadcast. Some devices may report their status at a regular interval, while others only report in response to a request broadcast, and others may communicate by both methods. In essence, the CAN bus data stream consists of a sequence of (key, value) pairs.

Fleet Carma’s logger has a list of parameter identifier (PID) values that are to be collected from the OBD2 system. Whenever any of those PIDs appear on the CAN bus, the logger records and timestamps it. To ensure a data log meeting the specified resolution requirements (1 second while moving), the logger periodically sends update requests for over the CAN bus for appropriate PIDs, requesting that a new value be returned.

The problem derives from the logger’s conversion of the sequential stream of PID-value pairs, into an analyst-friendly timeseries table format, with one row per timestamp and one column per PID. In this conversion, a row is generated shortly after an updated value is received over the CAN bus. Unfortunately, any PIDs which have *not* reported updated values appear to have been assigned *their last known value* for a given row. Table 4 presents an exaggerated illustration of the problem, showing how a reasonable acceleration to 5  $m/s$  over 10s could generate an apparent acceleration of 50  $m/s^2$  :

Table 4: OBD2 Log Problem Example

Seconds	$\Delta T$	CAN message	MAF ( $g/s$ )	Speed ( $m/s$ )	Acceleration ( $m/s^2$ )
30.0	-	speed=0	4.3	0	-
30.1	0.1	MAF=11.3	11.3	0	0
39.9	9.8	MAF=10.9	10.9	0	0
40.0	0.1	speed=5	10.9	5	50

### 2.3.2 Fuel vs airflow

Unfortunately, a parameter for fuel-flow rate is not part of the OBD2 specification [52]. Most vehicle manufacturers supply a proprietary PID for this value, but our FleetCarma loggers were not configured to retrieve it from the individual vehicles. A valuable proxy for fuel flow is the standard PID mass-airflow (MAF), which estimates the mass of air entering the engine from measurements of airstream temperature and velocity at the intake. The well-known stoichiometric mass ratio of 14.7 for gasoline combustion is inferred from the oxidation reaction [53]:



Since tailpipe emissions are an important design consideration, modern vehicles attempt to minimize emissions by ensuring good operation of the catalytic converter. One outcome of this intent is that the vehicle continually modifies its fuel flow (a process referred to as *trimming*) relative to MAF, in order to maintain clean combustion as indicated by the oxygen content of the exhaust stream. There *do* exist standard PIDs for both the commanded and measured ratios of fuel to air [52], but these values were unavailable to this study, having not been logged in the CRD's Smart Fleet project.

In any case, a properly operating vehicle should generally have a fuel flow within 10% of the stoichiometric ratio relative to the MAF [54]. It is noteworthy that there are certain events (notably engine-braking) that will be expected to cause significant transient departures from the stoichiometric ratio. The author's personal experience, having reviewed trim data logs from five personal vehicles, is that short and long-term fuel trim levels generally remain consistent within 3% for normal driving, outside of a few minutes for engine warm-up.

The conclusion from this background material is that calculating fuel flow by applying the stoichiometric ratio of 14.7 to the measured MAF can be reasonably expected to have a *per-vehicle precision* of  $\pm 3\%$ , and an *absolute accuracy* within  $\pm 10\%$ .

Ultimately, the MAF estimate must stand alone as a ground truth for this work, as no means of validating the MAF estimate was found. The CRD does track fleet fuel consumption under BC's Climate Action Revenue Incentive Program (CARIP) program, but not in a manner that could be isolated to specific vehicles, or even to the subset of vehicles under observation. A project was underway to implement a card system that will ultimately track the fuel consumption of individual vehicles, but no data was available for the study period.

## 3 Data Cleaning and Preparation

3.1 Raw Data . . . . .	27	3.2.3 Stop-start errors . . . . .	31
3.1.1 Collection . . . . .	27	3.2.4 Other errors . . . . .	32
3.1.2 Parsing and selection . . . . .	27	3.3 Power Data Cleaning . . . . .	32
3.1.3 Feature selection . . . . .	29	3.3.1 ICE power . . . . .	32
3.2 Speed Data Cleaning . . . . .	30	3.3.2 BEV power . . . . .	32
3.2.1 Speed data problems . . . . .	30	3.4 Regularization . . . . .	35
3.2.2 Recurrent speeds . . . . .	30		

This section describes the process required to make the timeseries logger data ready for segmentation and fingerprinting. This was a key and challenging element of the research, requiring approximately 4000 lines of python code.

### 3.1 Raw Data

#### 3.1.1 Collection

As discussed above, the CRD’s ZEFI project [7] included telematic loggers installed in fleet vehicles for approximately a year starting in early 2018. Summary statistics of the data collection effort are shown in table 5, with the distribution of samples between vehicle-missions shown in figure 3.

The loggers were capable of logging and transmitting global positioning system (GPS) locations and a collection of engine data parameters that differed from vehicle to vehicle, but which always included speedometer (wheel) speed. FleetCarma was asked to collect fuel flow rates, but as this is not part of the OBD2 standard, FleetCarma instead collected various proxies for fuel flow, primarily MAF and AbsLoad.

#### 3.1.2 Parsing and selection

The raw logger data was received in one text file per trip, where trips comprised periods of time where the logger was supplied with accessory power from the host vehicle. The

Table 5: Data Collection Statistics

Feature	Value
Total vehicles	55
Total samples	18356982
Study vehicles	29
Study samples	10617365
First datum	2018-01-29
Last datum	2019-02-20

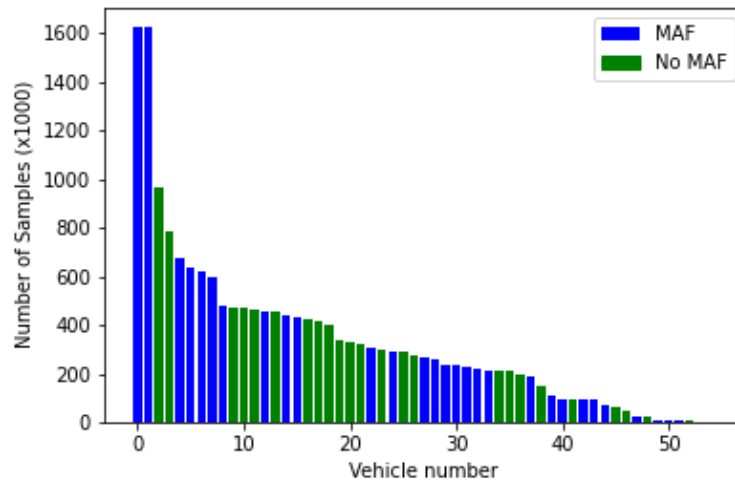
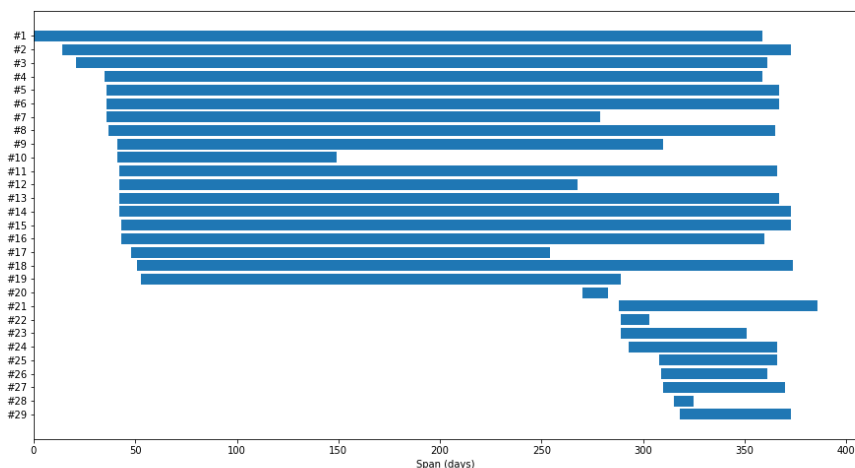


Figure 3: Sample counts by vehicle, studied and non-studied



*Figure 4: Data collection timespans for individual vehicles*

files were in comma-separated-value (CSV) format, indexed by time or time-offset (one row per timestamp, one column per sensor), but did not use consistent file-formats, units, column selections, nor column naming conventions, so ingestion of the data into a standard format was a challenging and time-consuming task.

Only about half of the ICE study vehicles were configured to log MAF. The OBD2 PID AbsLoad was provided for the remainder, but this is not a proxy for fuel consumption without reference to engine revolutions per minute (RPM), which was not collected. ICE vehicles without MAF were therefore eliminated from the study group. This was a significant and disappointing setback, and a stern reminder to attempt a limited model proof of concept early in the data collection process. However, the remaining data is sufficient in breadth and depth to demonstrate the core thesis, albeit not so clearly shown to generalize across many different vehicle and mission types.

The various vehicles were monitored for different time periods, with the length of their study period shown in figure 4.

### 3.1.3 Feature selection

The complete list of attribute names collected by the various loggers is listed in appendix A, table 14. Several of these features are duplicated with alternate names – e.g., Speed

and Signal #131 are synonymous. For this work, only various aspects of vehicle speed (including vertical speed, from GPS altitude) and derived variables were selected as features, with a target feature of vehicle energy consumption – derived from MAF on ICE vehicles, and primarily state of charge (SOC) for BEVs.

## 3.2 Speed Data Cleaning

### 3.2.1 Speed data problems

Various statistics related to vehicle acceleration were of primary interest to this study. Accelerations were trivially computed from the measured timeseries speed logs for each trip, but examination showed a large fraction of impossibly high accelerations.

It seems well-accepted that consumer-grade tires on dry pavement offer a peak static friction coefficient of around 0.7 [55], so all acceleration values in excess of  $0.7 \times 9.8 = 6.9 \frac{m}{s^2}$  are suspect. About 132k (or 1.25%) of the 10.6M speed samples implied accelerations above this threshold. Examination of the log data showed 56.2% of log speed values were unchanged from the previous value, suggesting “sticky” sensor readings at the OBD2 logger, as described in section §2.3.1.

Since statistics derived from vehicle acceleration comprise the primary features to be investigated for fingerprinting travel segments, it was of critical importance to remediate the speed data collection/integration errors and restore a true reflection of the vehicles’ speed and acceleration profiles prior to attempting analysis. This section explains how the speed data was cleaned.

### 3.2.2 Recurrent speeds

Since the speed of a moving vehicle is inherently variable, nonzero speed values should only recur very infrequently. It seems obvious that a large fraction of the recurring values are invalid data integration artifacts. In the absence of any information about *which* recurrent speed values happened to be valid, the author elected to eliminate all of

Table 6: Impact of data cleaning methods on rate of "impossible acceleration" errors

	Samples	Errors	Error Rate (%)	Error reduction (%)
Rows removed				
Nil	10,617,365	132,291	1.25	NaN
Moving recurrent	7,874,102	12,727	0.162	90.4
Impossible starts	7,861,375	69	0.000878	99.5

them. This substantially improved the quality of the data – that is to say, the deletions removed most of the invalid acceleration values. The number of valid data points also deleted is believed to be very small, and in aggregate likely to do little harm for the purpose of this study. The obvious exception is made for periods of zero speed, where it was to be expected that the vehicle’s zero speed was indeed constant for some period of time.

Accordingly, all recurrent speed samples were deleted, except for zero-speed samples. This deletion reduced the number of samples by almost 1/3, but reduced the number of impossible acceleration events from 132k to 12k – a reduction of 91.4%.

A summary of the reduction in error rates from data cleaning is shown in table 6

### 3.2.3 Stop-start errors

Of these remaining impossible acceleration events, nearly all occur during vehicle starts – samples where the previous speed was zero.

This comprises an error rate of 5.01% during starts from zero speed. Examination of the offending high-acceleration samples reveals an extraordinarily high number of short (sub-second) intervals after the final zero-speed sample. This strongly implies that these accelerations are another artifact of the “sticky” value problem discussed in section 2.3.1.

In the interest of simplicity, these roughly 12,000 impossible-start samples were dropped. Since the way a vehicle is started may have useful predictive power (e.g., jackrabbit

starts), future work should be applied to recovering the information in start samples, as discussed in section 7.2.1.

### 3.2.4 Other errors

With the above cleaning methods applied, the corpus contained only 69 remaining samples with impossibly high acceleration values. Inspection showed these to generally correspond to high rates of change over short sample periods, but with no obvious cause. These samples could very well be true values, perhaps due to wheels spinning under high power or wheel-lockup due to hard braking. These samples have been left intact.

## 3.3 Power Data Cleaning

Again, the core problem of this thesis is to predict each vehicle's characteristic input power for each eigentrip. The model's ground truth will be the input power consumed during each trip segment, so a new power feature was calculated from the available features.

### 3.3.1 ICE power

For ICE vehicles, the energy input is fuel consumed. Fuel consumption was approximated from logged MAF at the stoichiometric fuel:air ratio, an assumption discussed in §2.3.2 and §7.1. The energy value was then calculated using the LHV of  $46.4 \frac{MJ}{kg}$  [56].

The MAF PID suffered from the same "stickiness" problem as the other PIDs discussed above, and had an effective sample period of about 2 s. This was addressed by the same means as for speed: removing all recurrent values, except zero-value periods.

### 3.3.2 BEV power

For the BEVs, input power is from the high-voltage (HV) main drive battery.

Although FleetCarma attempted to provide 1-second resolution power data, the data suffered from the same stickiness problem as elsewhere; the real sampling rate was much lower than expected. SOC was sampled at a median period of 87 s, HV battery current at 29 s, and HV battery voltage at 30 s. This low sampling frequency complicated the power calculation; multiplying spot-sampled voltage and current with the elapsed time would miss transient events, and be unlikely to provide an accurate reflection of total consumption. Reported SOC is not perfectly suitable, being unlikely to have been sampled near a given segment boundary.

A rejected course of investigation was to interpolate SOC along the better-sampled HV voltage reading, on the assumption that battery voltage would drop linearly with expended energy. Plots of SOC vs voltage for multiple trips (figure 5) suggested that there is a good relationship between these features. However, inspection of a number of actual time-domain plots of battery voltage and SOC similar to figure 6 suggest that the correlation only exists reliably at a scale too broad to be of practical use.

As shown in figure 6, the HV system’s voltage readings are highly variable while the vehicle is in motion; this reading shows system voltage rather than open-circuit battery voltage. Furthermore, the system’s logging resolution is far too low to estimate energy consumption (E) from voltage (V) and amperage (I) in the typical manner, as:

$$\Delta E = \int V(t) \times I(t) dt \quad (6)$$

Fortunately the vehicle’s on-board computer has high-resolution access to the electrical sensors, and can make use of a combination of several methods for establishing the remaining useful charge in the battery [57]. SOC is therefore a reasonably trustworthy absolute measurement relative to the vehicle’s known battery pack capacity, and a reasonable estimate of energy consumption over time can be obtained from it.

Ultimately, no better method was found than applying vehicle-reported SOC to manufacturer-published battery capacity of 27 kWh for the Kia Souls [58, 59], and 12 kWh for the Outlander PHEV [60]. This required linear interpolation of SOC to the

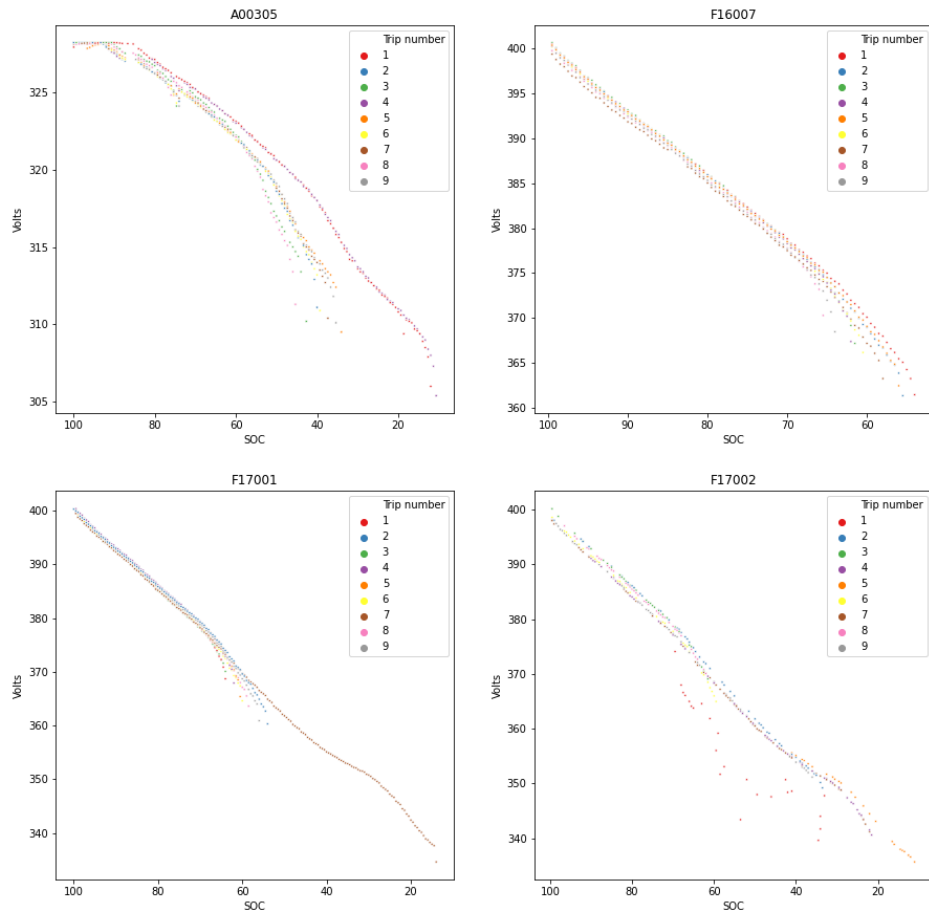


Figure 5: EV example trips showing the broad relationship of SOC vs the main battery's voltage

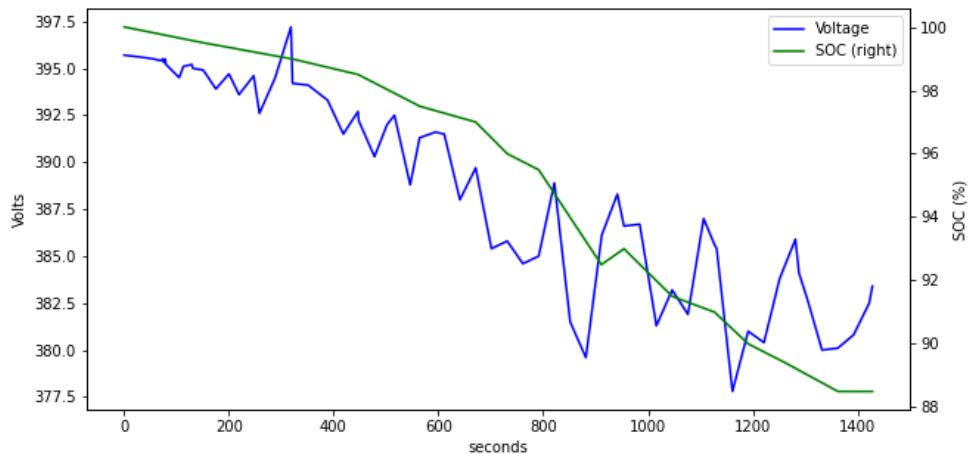


Figure 6: One EV example trip showing the rapid changes of voltage readings over time

Table 7: Number of samples and trips removed by EV data cleaning procedures

	EV Samples	Removed	EV Trips
Nil	817,820	0	2,308
Zero power	817,641	179	2,181
Charging	796,022	21,619	1,762
Zero-time	796,022	0	1,762

segment boundaries as described below in §3.4, a significant assumption that merits the future work discussed in §7.2.3. Given these assumptions, energy used in a period is then simply:

$$\Delta E = \Delta SOC \times Capacity \quad (7)$$

Inspection of the power thus calculated showed a large number of null SOC and V-I measurements. Nearly all of these were addressed by deleting a small number of unusable data-logs, presumed to represent data collection artifacts generated by loggers not well-configured for their host BEVs, described in table 7.

### 3.4 Regularization

In order to reduce the amount of data uploaded over the cellular devices, the supplier configured their loggers to use a sample period of about 1 second while moving, and 30 seconds while stopped. After collection was complete, the "sticky" problem discussed in §2.3.1 was discovered, and with it the realization that various sensor values were recorded at different frequencies, and at fractional-second offsets from each other. The above process of removing recurrent values adequately eliminated the spurious readings, but introduced two distinct problems:

1. The longer-than-expected sampling period introduces complexity in handling segment boundaries – the final sample in each segment must be extrapolated across the boundary in order to be included in the second segment.
2. the sample following a 'stopped' sample may have a non-zero speed; barring the

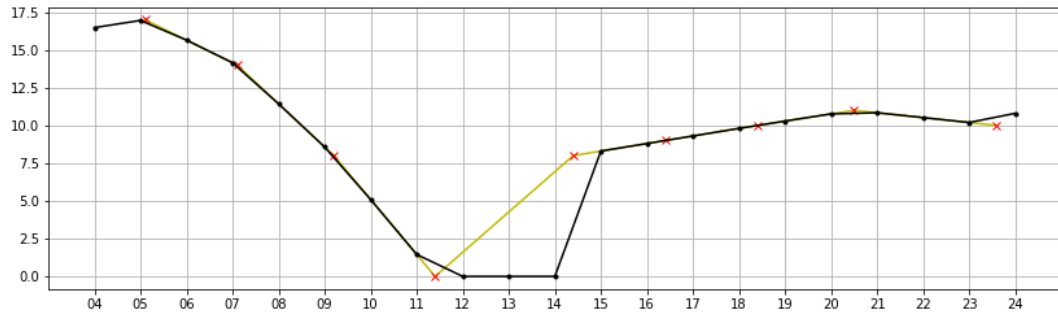


Figure 7: Problems caused by linear sample interpolation with and without regularization

introduction of synthetic 0-speed samples to terminate each stop, point-wise interpolation would result in apparent movement during the stop period. This is illustrated in figure 7, with sample points in red, direct interpolation in yellow, and the regularized interpolation shown in black.

To address these problems, the entire dataset was regularized to uniform 1s intervals, zeroed to clock time. I.e., regularized timestamps are at even multiples of 1 second from the top of the hour, rather than from the beginning of the trip, which would likely have been offset by a fractional second. Zero-speed periods were forward-filled to 1s intervals, and all in-motion data was linearly interpolated onto the regularized 1s interval.

# 4 Methodology

4.1	Feature Preparation . . . . .	37	4.3.5	LightGBM . . . . .	47
4.1.1	Segmentation . . . . .	37	4.4	Classification Method . . . . .	48
4.1.2	Feature values . . . . .	38	4.4.1	Wrong-class error . . . . .	48
4.1.3	Assumptions . . . . .	39	4.5	Energy Prediction . . . . .	49
4.1.4	Data review . . . . .	39	4.6	Parameter Refinement . . . . .	50
4.2	Clustering . . . . .	41	4.6.1	First pass iteration . . . . .	50
4.2.1	Intent . . . . .	41	4.6.2	Second pass iteration . . . . .	51
4.2.2	Key insight . . . . .	42	4.6.3	Hyperparameter tuning . . . . .	51
4.2.3	Cluster visualization . . . . .	42	4.6.4	Interpretation and parameter selection . . . . .	52
4.3	Classification Algorithm . . . . .	42	4.7	Comparison Predictions . . . . .	55
4.3.1	Algorithm selection . . . . .	42	4.7.1	Published fuel economy . . . . .	55
4.3.2	Decision Trees . . . . .	44	4.7.2	LGBM regression . . . . .	55
4.3.3	Boosting and AdaBoost . . . . .	45			
4.3.4	Gradient Boosting Machines . . . . .	46			

This section describes the process chosen to build a spreadsheet-compatible energy prediction model from the cleaned timeseries logger data. In broad terms, the steps were as follows:

- Divide travel data into segments
- Compute kinetic fingerprint features and average power
- Select reasonable starting clustering parameters
- Cluster into groups representing eigentrips
- Characterize missions by classifying travel data
- Iteratively refine clustering parameters and model hyperparameters

## 4.1 Feature Preparation

### 4.1.1 Segmentation

As in Wu’s drive cycle classifier [31], the data was consolidated into 3-minute segments to match the resolution of a typical urban stop-go-stop cycle. The resampling is relative

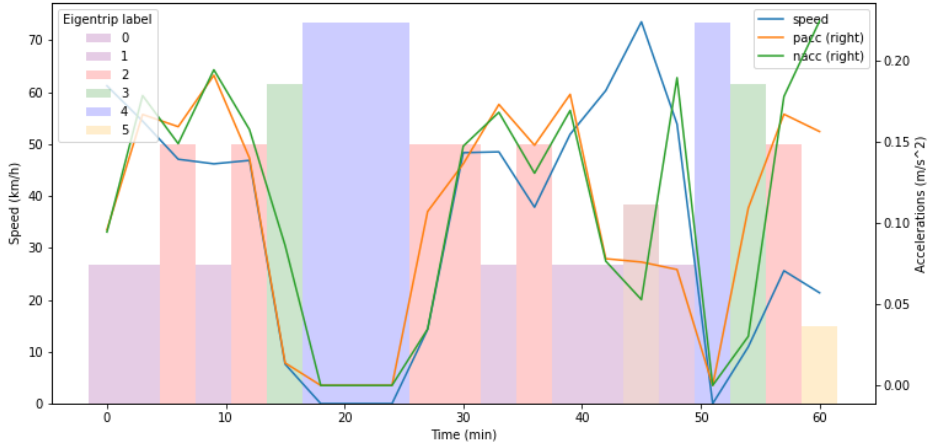


Figure 8: Timeseries trace of speed and accelerations, overlaid with eigentrip labels

to the top of the hour (IE, segments begin and end at even multiples of 3 minutes past the hour). This has the advantages of consistency and simplicity with the tools at hand, but it also results in the first and last segment of each trip having shorter durations. E.g., if a trip began at 15:02:15, its first segment will end at 15:02:59 for a duration of only 45 seconds.

The fixed segment duration, the choice of 3-minute segments, and the clock-time interval boundaries are all assumptions meriting further investigation as discussed in §7.3.4 and §7.3.5.

An example period of travel is shown in in figure 8, with a timeseries plot of the average speed, acceleration, and deceleration values in each 3-minute segment. The plot segments are superimposed on blocks representing their eigentrip labels, to give a sense of the decomposition process.

#### 4.1.2 Feature values

For each 3-minute segment, Wu’s vehicle-independent trip features [31] were computed, including averages and maximums for speed, acceleration, and deceleration, as well as the fraction of time spent idling (see table 2).

One oversight in Wu’s choice of features is road grade – a significant factor in short-term power requirements. Fully 42% of the data collected in this study lacked GPS altitude,

and of the non-null data, 61% were repeat values. Where possible however, positive and negative vertical speed features were calculated. To give some insight into regenerative braking, an additional feature was computed from the count of acceleration reversals – the number of times the vehicle changed from acceleration to deceleration, or vice versa.

Each travel segment was additionally labelled with its mean input power in kW. The derivation of power from the available log data is described in detail above in §3.3. In brief, ICEV power is derived from MAF at the stoichiometric ratio, and BEV power from the time-interpolated SOC.

### 4.1.3 Assumptions

Refining and simplifying assumptions were applied to the feature calculations as follows:

- Null samples indicate that either the logger or CANbus is inactive, which should typically only happen when the vehicle is at rest and/or the engine is stopped. Null values were therefore presumed to indicate zero speed and/or energy consumption.
- For maximum values, the 98th percentile (Q98) value was selected to minimize the effect of outliers and incorrectly captured values.
- In spite of using a quantile for maximums, the mean was used to represent average, since the other measures of central tendency minimize the informational effect of skewness, which is valuable here.
- Information doubly-represented in other statistics (eg, zero-speed samples, also captured in the idle-fraction statistic) was not excluded.

### 4.1.4 Data review

Histograms of the feature values plus power consumption rate are visualized stripped of outliers (beyond 2.5 IQR) in figure 9, and further stripped of the minimal value and maximal value in 10.

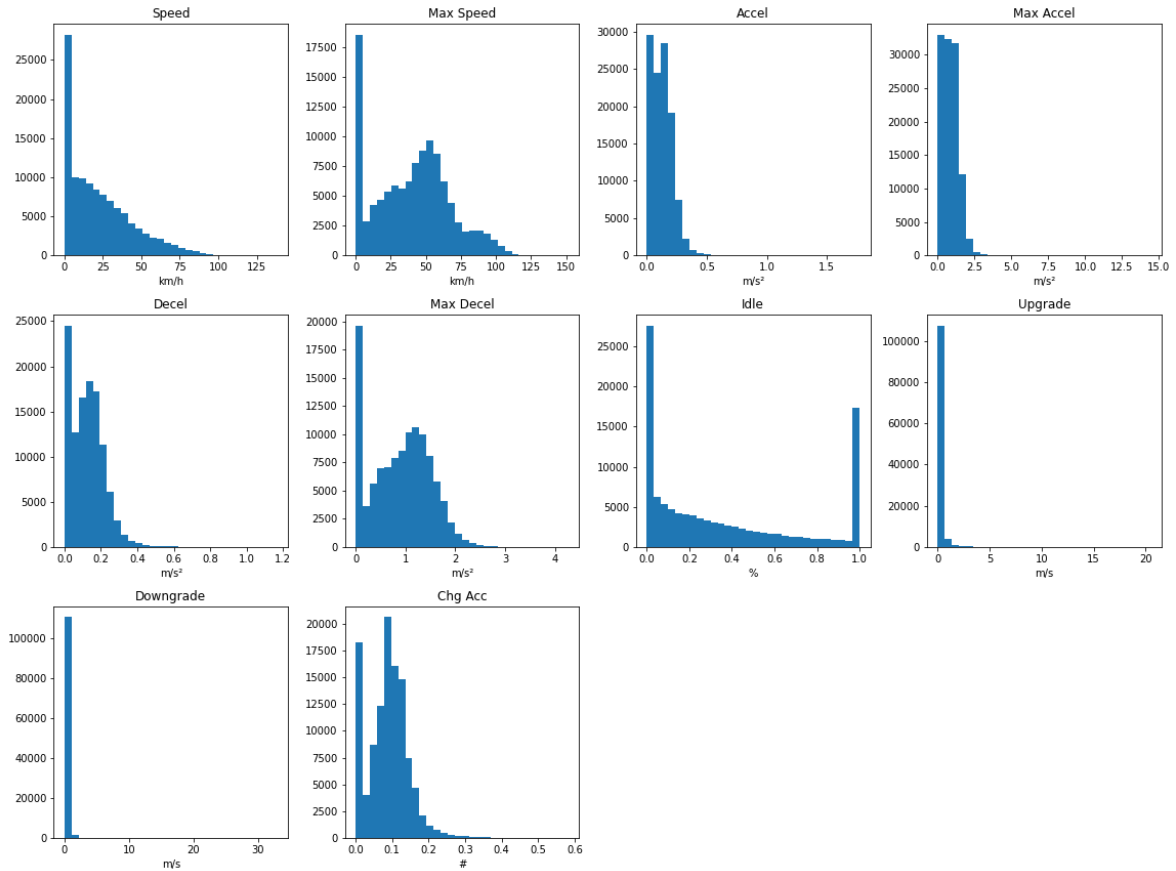


Figure 9: Feature value distributions, including end-of-range values

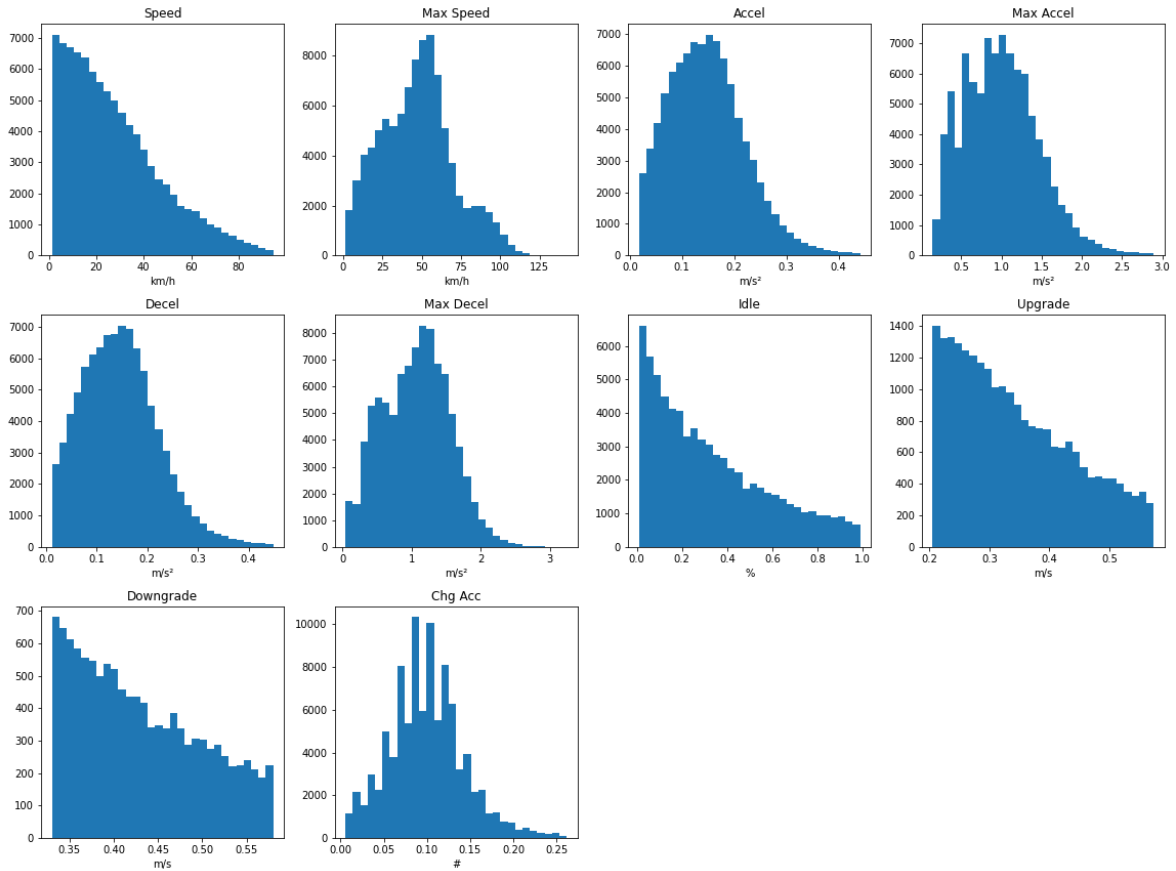


Figure 10: Feature value distributions after removing common end-of-range values

## 4.2 Clustering

Having established a clean corpus of fingerprinted travel segments, the next step was to perform a preliminary clustering of the segments into similar groups.

The individual features did not exhibit significant modalities other than those obviously caused by segments where the vehicle was idle; there is no reason to expect that the data is inherently clustered. Since the clusters will be selected arbitrarily to improve the model's performance, a simple clusterer using Euclidean distance suffices for initial validation. K-means clustering was chosen due to its simplicity and the fact that the Scikit-learn implementation does not scale its inputs, permitting feature weighting by scaling. Since K-means greedily minimizes within-cluster sum-of-squares [48],

$$\sum_{i=0}^n \min_{\mu_j \in C} (\|x_i - \mu_j\|^2) \quad (8)$$

it tends to result in clusters which are roughly spherical, rather than elongated or convex. This is a limiting factor deserving additional work (§7.4.1), but it does not prevent the technique from establishing reasonable cluster centroids, nor from providing labelled groups which will train a functional classifier.

### 4.2.1 Intent

The centroids of these groups define the characteristic travel-type exemplars that we are calling "eigentrips". The eigentrips are used to estimate a vehicle's input power according to the vehicle's type, and the kinetic characteristics of the travel it is undertaking. The goal is therefore to find a set of eigentrips, each of which represent a travel regime with both (a) consistent kinetic characteristics, and (b) similar input power within each vehicle type.

### 4.2.2 Key insight

It was desired that the eigentrips represent regimes of travel with similar power *within each vehicle-type*, but not necessarily *across* vehicle-types, so power was added as a feature for the purpose of clustering, and weighted to emphasize its importance relative to the individual kinetic features.

The inter-vehicle difference in power for a given travel-type would be a confounding factor, so the power feature is standardized to Mahalanobis distance (shifted to have a zero mean, and scaled to number of standard deviations) *separately for each vehicle*.

### 4.2.3 Cluster visualization

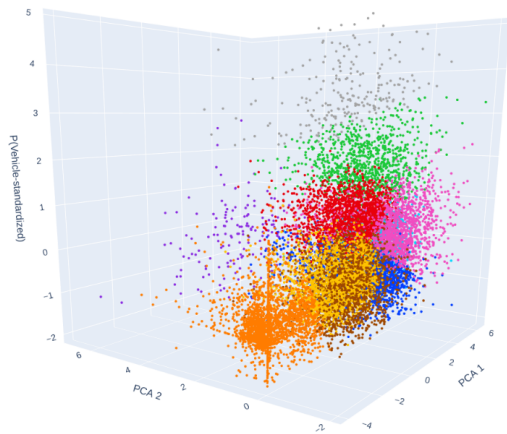
A preliminary K-means clustering operation was performed with K=10 clusters, and the power feature weighting increased by applying a power-scaling factor (PS) of 2.0. The kinetic features were reduced to 2 dimensions with PCA as shown in table 8. The PCA-reduced kinetic features were visualized on a 3D scatter plot, with the Z axis showing power, and the cluster labels differentiated by colour. Clustering for the complete training dataset is visualized in figure 11(a), with power standardized within each vehicle. The similar subfigure (b) shows the subset of data for a single vehicle, with non-standardized power.

## 4.3 Classification Algorithm

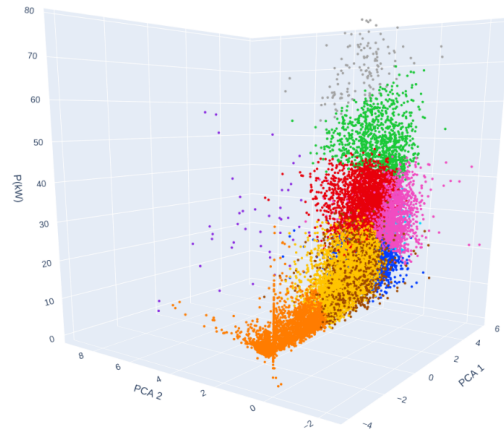
### 4.3.1 Algorithm selection

The core of the proposed model is the classification of travel segments by their kinetic features, and labelling them with the most-similar eigentrip. This label permits predicting a likely vehicle-specific characteristic power for the segment. In other words, the clustering process above has *defined* the eigentrips, and now they can be *applied*.

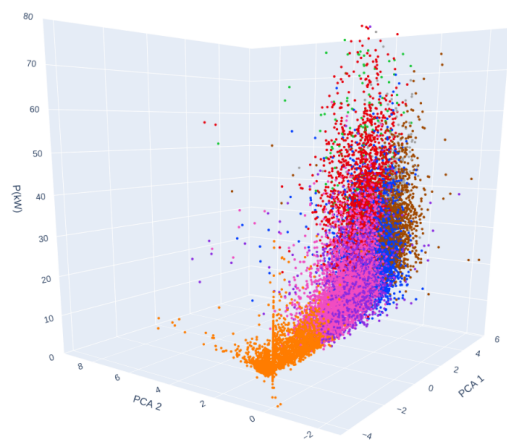
The feature histograms (figure 10) showed the bulk of feature data in well-ordered distributions, but many with a large additional peak at zero (as well as unity, in the case



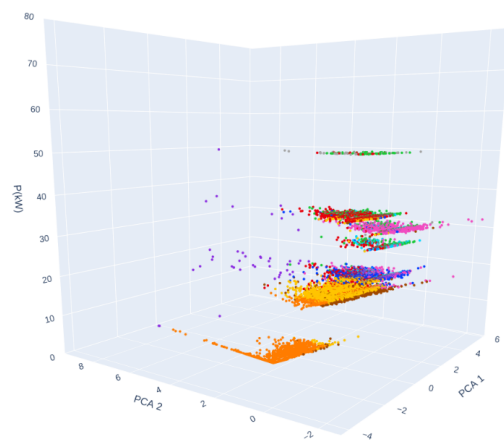
(a) Standardized power (all training data)



(b) Actual power



(c) Actual power, predicted labels



(d) Predicted characteristic power

Figure 11: Visualization of preliminary clustering ( $K=10$ ,  $PS=2$ ) and classification, as applied to one example vehicle

Table 8: PCA components for 2D visualization of kinetic features( $K=10$ ,  $PS=2$ )

	PCA 1	PCA 2
Speed	0.302	0.0828
Max speed	0.355	0.0551
Acceleration	0.372	-0.100
Max acceleration	0.342	-0.110
Deceleration	0.365	-0.0745
Max deceleration	0.368	-0.0778
Idle	-0.39	0.0139
Climb	0.0884	0.684
Descent	0.0878	0.692
Acceleration reversals	0.303	-0.0976

of the idle fraction feature). This modality means that parametric classifiers assuming a single distribution will be ill-suited. Since selecting cluster parameters required an iterative search of  $K$  (number of clusters) and  $PS$  (power-scaling) combinations, a fast classifier was desired.

The LightGBM classifier [61] meets these requirements. LightGBM is a gradient boosting framework, with several interesting optimizations. The remainder of §4.3 is a short introduction to some core concepts underlying the LightGBM model: decision trees, boosting, gradient boosting, and a short description of LightGBM’s optimizations.

### 4.3.2 Decision Trees

The simplest possible decision tree is a single inequality criterion that branches a dataset into two leaves. Figure 12 illustrates an example, letting records where feature #2  $\leq$  4.85 go into the *left* leaf, the remainder into the right.

Selecting the best choice for the split criterion requires a method of quantifying the "purity" of potential splits – the degree to which information is added by by creating the split. Shannon entropy, mis-classification error rate, and Gini impurity are common metrics for classification, and sum of squared error for regression [62, §9.2]. In the simplest illustration, every unique datum is examined as a split point, selecting the one which results in the lowest total impurity in its leaves.

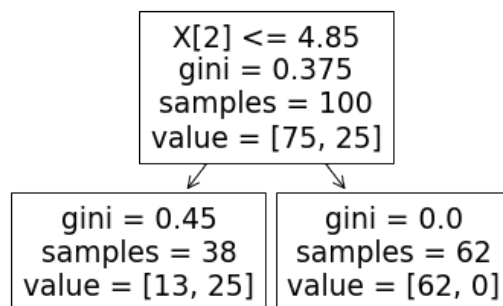


Figure 12: Example of a single-node decision tree, or "stump"

### 4.3.3 Boosting and AdaBoost

Gradient Boosting is the name for a group of methods for building an ensemble of "weak" learning machines (often small decision trees), each building on the weaknesses of its predecessors.

It is best illustrated with AdaBoost, the first adaptive boosting machine, and arguably the simplest and best-known [62]. The following pseudocode, derived from [63], uses the simplest possible real classifier (a decision tree stump) applied to an input dataset  $X$  with labels  $y$ .

1. Start by defining the first weak learner  $F_1$  (a decision tree stump, as discussed in §4.3.2), trained from the initial input dataset  $X_1 = X, y_1 = y$
2. Use the  $F_1$  to generate predictions  $\hat{y}_1$  against labels  $y_1$ .
3. Compute loss  $L_1$ . For classification, this might be the fractional error rate

$$L_1 = \frac{1}{N} \sum |\hat{y} \neq y| \quad (9)$$

4. Compute *performance value*  $\alpha_1$ , a number that is larger if the classifier performs well.

$$\alpha_1 = 0.5 \log\left(\frac{1 - L_1}{L_1}\right) \quad (10)$$

5. Halt iteration if stop conditions met (e.g. a predetermined number of iterations).

6. Create a new input dataset  $X_2, y_2$ , with a larger proportion of records incorrectly classified by  $L_1$ . Selection is pseudo-random, using a weight vector

$$w_2 = e^{-\alpha_1 s_1} \quad (11)$$

$$\text{where } s_1 = \begin{cases} 1, \hat{y}_1 = y_1 \\ -1, \hat{y}_1 \neq y_1 \end{cases} \quad (12)$$

7. Train a new tree  $F_2$  from the new dataset  $X_2, y_2$ , and iterate from step 2.

The final classification decision takes the form of a weighted vote between the weak learners, weighted by each learner's performance metric  $\alpha_i$ .

#### 4.3.4 Gradient Boosting Machines

Gradient Boosting Machines are a generalization of the AdaBoost concept, allowing different loss functions, and applying a kind of gradient descent in order to reduce error in a smaller number of iterations. A gradient boost model is superficially similar to AdaBoost, in that it consists of an ensemble of weighted weak learners:

$$F(X) = F_0(X) + F_1(X) + \dots + F_m(X) \quad (13)$$

$$\text{where } \begin{cases} F_i = \gamma_i r_i \\ r_i = -g(L)|_{i-1} \text{ (negative gradient of loss function)} \\ \gamma_i = \underset{\gamma}{\operatorname{argmin}} L(F_{i-1} + \gamma r_i) \end{cases} \quad (14)$$

Where  $\gamma_i$  are weights and  $r_i$  are the pseudo-residuals of the preceding weak learners. In essence, each element  $F_m$  is the output of a decision tree trained to predict the pseudo-residual  $r_m$ . In the special case where the loss function is sum of squared errors (SSE), this is the (true) residual of the prior elements. The output is then scaled by a weighting factor  $\gamma_m$ , selected to minimize the overall loss.

In other words, gradient boosting is conceptually different from AdaBoost in that each

element  $F_i$  is a weak learner tuned to directly address a pseudo-residual – an incremental step in the direction of steepest improvement in the loss function. In other words, the gradient of loss  $L$  with respect to the prediction  $F$ :  $\frac{\delta L}{\delta F}$  [62, §10.10].

Unsurprisingly, nearly every teaching example (e.g. [64]) of gradient boosting tends to use the same, extremely convenient loss function; the one which produces the simplest gradient:

$$L_i = \frac{1}{2}(y - \hat{y}_i)^2 \quad (15)$$

$$\text{so... } r_i = - \frac{\delta L_i(X)}{\delta F_i(X)} = \hat{y}_i - y \quad (16)$$

Additional weak learners are added until a stop condition is met, typically either (a) a specified number of estimators have been added, or (b) the loss has been reduced to an acceptable threshold.

#### 4.3.5 LightGBM

The Light Gradient Boosting Machine (LGBM) is a framework for applying gradient-boosted decision trees (a specialization of GBM where the weak learners are always small decision trees), with a number of optimizations to improve training speed and improve accuracy [65]. In particular, it provides the following [66]:

- gradient-based one-side sampling (GOSS) histogram split finding: an alternative method of tree construction which finds high-performance splits very quickly by keeping high-gradient rows, as well as samples from rows with small gradients
- exclusive feature bundling (EFB), allowing sparse, mutually exclusive features (IE, those with few overlapping nonzero values) to be grouped into a single feature for split evaluation
- best-first tree training; for a given maximum number of leaves, this method often improves overall accuracy by splitting the leaf which most reduces loss
- bagging, helpful to reduce variance [62], and implicitly to reduce the likelihood of over-fitting

## 4.4 Classification Method

An LGBM classifier was constructed by training with the kinetic features using 10% of the labelled data for each vehicle, with the remaining 90% held back for testing. This method is at odds with the apparent industry standard method of 80% training / 20% hold-back, but given a reasonable quantity of data, a small, well-distributed training set in conjunction with extensive testing serves to ensure that the model is generalizable and not over-fitted.

Figure 11 shows the results of classification on the sample vehicle. Subfigure (c) shows the eigentrip label (colour) of each segment predicted by the classifier solely with reference to the kinetic parameters, and subfigure (d) shows the as-clustered original labels, but with the predicted power.

### 4.4.1 Wrong-class error

In general, a multi-class classifier returns the set of probabilities that a given element (in this case, a travel segment) belongs to each possible class (in this case, the various eigentrips). Typically, the class with the highest probability (the *maximum likelihood* class) is selected. Applying this technique, the trained classifier had a label selection accuracy of 77.9%. The misclassification rate is not as concerning as it might seem: since the dataset is not in distinct clusters, segments of indeterminate class can be expected to have an actual power somewhere between the characteristic powers of its most probable classes.

It seems possible that the correct power may often fall between the highest and second-highest probability classifications. A refinement for future work (discussed in §7.4.2) is for cases where membership is unclear, to attempt selecting the two most probable classes, and pro-rating the segment's eigentrip membership by probability.

## 4.5 Energy Prediction

For the purpose of energy prediction, each travel segment is represented as a time-weighted vector, where each element represents a time-weighted (and potentially probability-weighted) count of eigentrips. E.g., if the segment is 180s long, and is best represented by eigentrip  $e_2$ , the segment is now represented by  $\mathbf{S} = [0, 180, 0, 0, \dots]$ , where the elements of  $\mathbf{S}$  represent the number of seconds spent in each of the eigentrip types. Any period of travel ( $\mathbf{T}$ ) can now be represented as the sum of its segment vectors:

$$\mathbf{T} = \sum \mathbf{S}_i \quad (17)$$

Given a vehicle's list of characteristic power values for each eigentrip  $\mathbf{C}_v = [P_{v,e1}, P_{v,e2}, \dots]$ , the predicted energy consumption for that travel is:

$$E = \mathbf{T} \cdot \mathbf{C}_v \quad (18)$$

Accuracy is assessed relative to the logger estimate of observed power for any given period of travel, in terms of modified mean absolute percentage error (MMAPE):

$$MMAPE = \frac{100\%}{n} \sum_{t=1}^n \left| \frac{y_t - \hat{y}_t}{1 + y_t} \right| \quad (19)$$

This initial model configuration (K=10, PS=2) exhibited a per-segment MMAPE of 37.4%, somewhat better than the baseline prediction error of 50.9%, calculated below in §5.

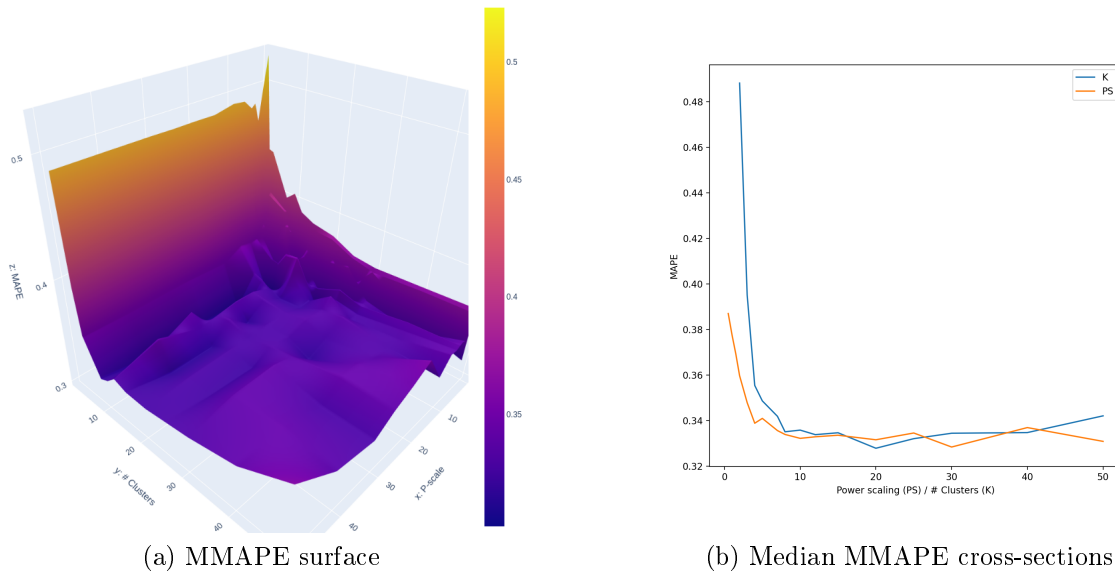


Figure 13: Two visualizations of prediction error (MMAPE) versus a broad selection of number of clusters ( $K$ ) and power-scaling factor ( $PS$ )

## 4.6 Parameter Refinement

### 4.6.1 First pass iteration

Having elected to cluster by K-means with a weighted power feature and demonstrated a process, the next step was to select (a) an appropriate number of clusters ( $K$ ), and (b) appropriate weighting with power-scale ( $PS$ ).

A number of values for  $K$  and  $PS$  were evaluated by clustering at each combination, and generating a prediction of average segment power to each configuration as described in §4.4 and §4.5. The MMAPE was calculated for each configuration, shown in figure 13(a). For clarity, the median of MMAPE values at various levels of  $PS$  is plotted for each value of  $K$  and vice-versa in (b). The figures show substantial random-appearing variation in error as  $PS$  is increased, presumably the result of classification error as the importance of the kinetic features in the clusters is reduced by over-weighting the power feature.

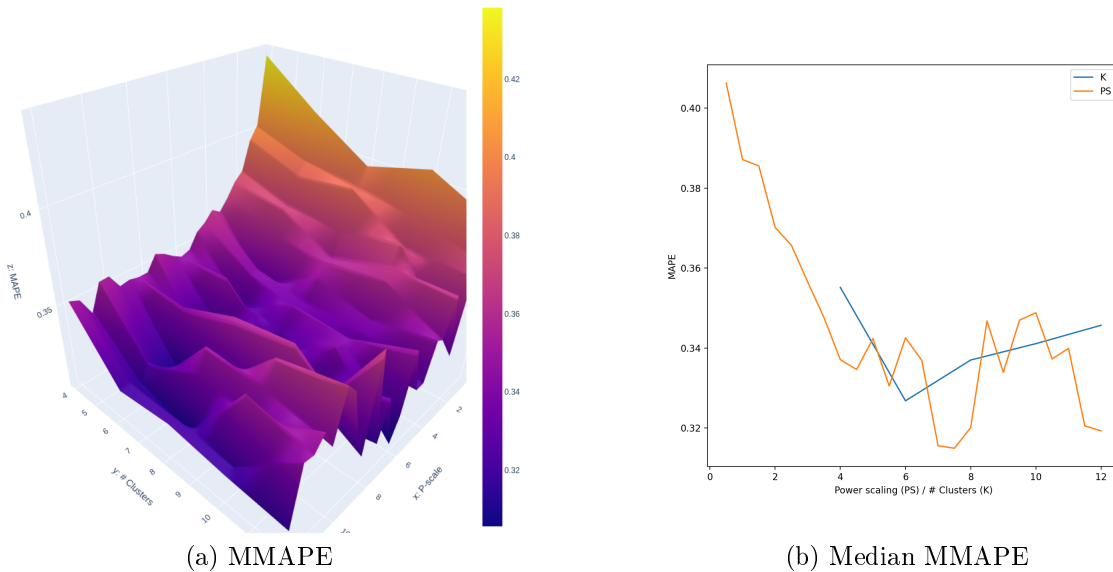


Figure 14: Local visualizations of prediction error (MMAPE) versus a narrowed selection of number of clusters ( $K$ ) and power-scaling factor ( $PS$ )

Table 9: LGBM hyperparameters selected for optimization

Hyperparameter	Value
bagging fraction	0.800
feature fraction	0.900
learning rate	0.0100
max bin	60.0
max depth	27.0
min data in leaf	39.0
min sum hessian in leaf	59.0
num leaves	80.0
subsample	0.0100

#### 4.6.2 Second pass iteration

Noise notwithstanding, the figures show a significant drop in MMAPE in the vicinity of  $K=8$  and  $PS=5$ , so a smaller-scale, higher-resolution iteration was performed in those regions (figure 14).

#### 4.6.3 Hyperparameter tuning

As with most ML algorithms, LGBM uses data-nonspecific settings called hyperparameters, which must be adjusted for best performance with the specific application.

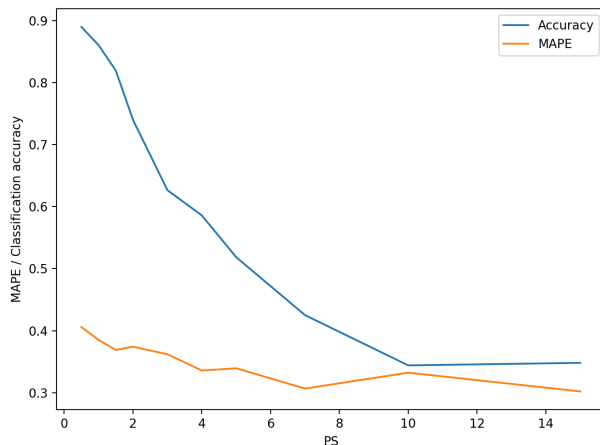


Figure 15: Prediction error and Classification Accuracy for various values of power-scaling factor (PS) with 10 clusters ( $K=10$ )

It is common to select these by iteratively testing the cross-validated performance of various values, and selecting the set which reliably perform best. A popular method is implemented in Fernando Nogueira’s optimization toolkit [67], which employs an evolving Bayesian process to home in on a likely minimum value for the loss function in a shorter number of steps than required by an exhaustive grid search. The technique is not central to this research; a simple grid search would return similar results at the cost of time. However, the implementation details are interesting and well illustrated in the author’s github page [68], with an application to LGBM published to Kaggle by Somang Han [69]. The application of this technique resulted in the hyperparameters shown in table 9.

#### 4.6.4 Interpretation and parameter selection

A deterministic optimization could be employed to find an absolute minimum MMAPE, but since the results would vary with every new random draw of training data, the improvement would not be persistent. Instead, parameters were selected from the region of the plot which appeared to best balance low MMAPE with low randomness. 10 clusters was chosen as a starting point due to the visible trough on the 3D surface plot.

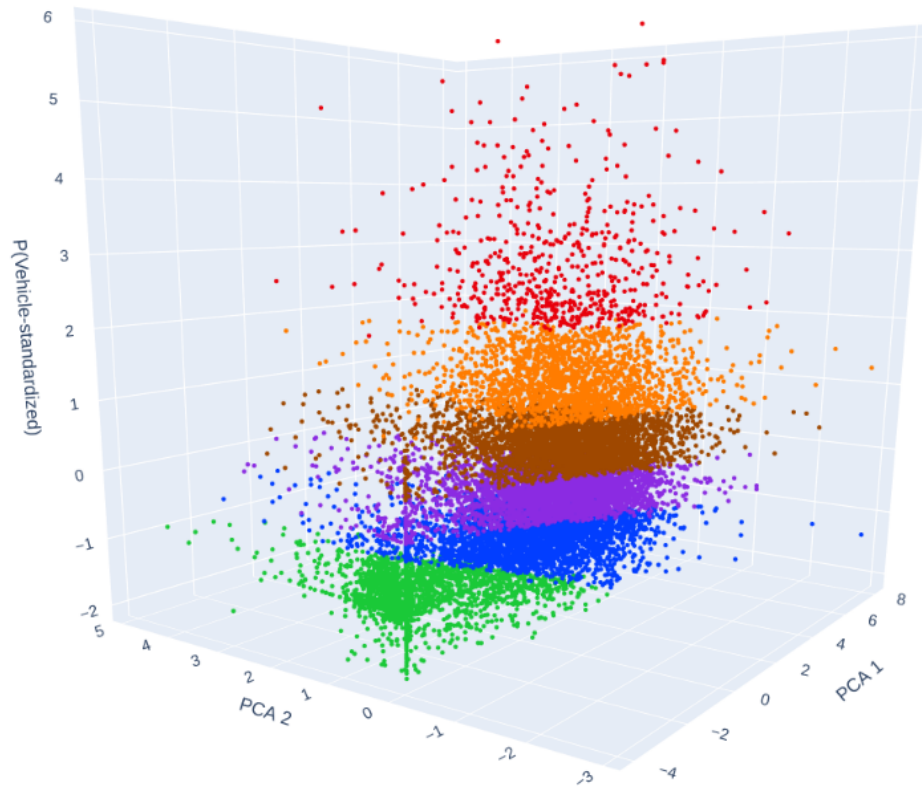


Figure 16: Final clustering ( $K=6$   $PS=7$ ), PCA kinetic features, and power

Classification accuracy and MMAPE were plotted at various values of PS that number of clusters, with results shown in figure 15. As desired, the increase in PS initially improves MMAPE, as clusters are defined with less internal scatter with respect to power. Classification accuracy drops rapidly with increasing PS, as clusters are defined which cannot be recalled without reference to the power feature, quickly overriding the improved prediction accuracy.

The final clustering with  $K=6$  and  $PS=7$  is visualized in figure 16. The noteworthy visual difference relative to the original clustering is that at the same visual Z-axis scale, the clusters appear "pancaked" – this reflects the desired stratification according to power levels. It is important to remember that this is a visual artifact; in the 11-dimensional hyperspace where the clustering operation was performed, the cluster boundaries still approximate hyperspheres, much as a cluster of soap bubbles approximate spheres.

This final clustering also permits the calculation of characteristic power values for each vehicle. Figure 17 shows the spread of actual power observations sorted by their cluster (eigentrip) labels, and divided into the various vehicle categories.

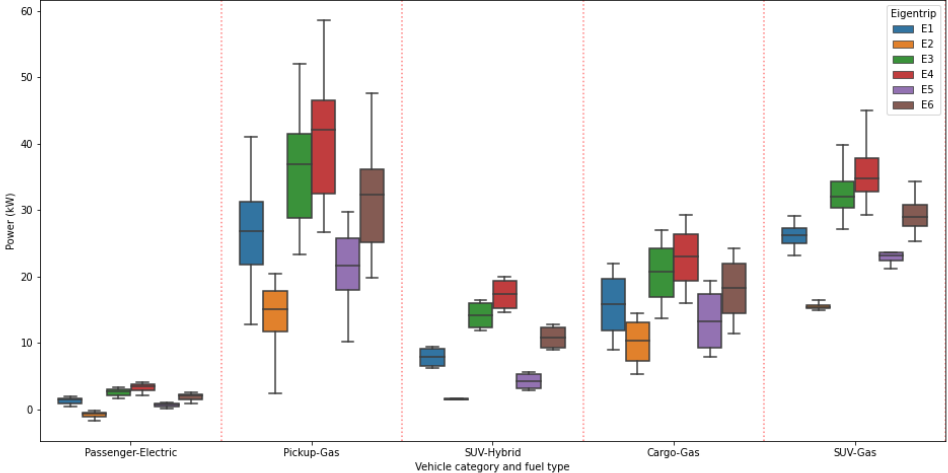


Figure 17: Power distribution of each vehicle category, as divided between the eigentrip labels

The average per-segment MMAPE of the eigentrips model was 32.3%.

## 4.7 Comparison Predictions

### 4.7.1 Published fuel economy

Business-as-usual (BAU) energy consumption prediction was established by applying published city/highway  $L_e/100km$  figures to the logged travel distances for each segment. The consumption test protocol [17] drive cycles had a mean speed of 34 km/h for city driving and 78 km/h for highway, so a dividing speed of 56 km/h was established midway between those means. Travel segments with an average speed at or below that dividing speed were predicted at the city figure, and those above predicted at the highway figure.

Fuel economy figures were selected for each vehicle with reference to NRCan’s fuel consumption rating search tool [70]. In each case, the base model was selected unless the CRD’s vehicle database indicated a specific sub-model or trim level.

The average per-segment MMAPE of this method was 50.9%.

### 4.7.2 LGBM regression

Finally, to establish the level of avoidable error with the information available to the model, a LightGBM regression model [66] was trained on the 10 kinetic features, as well as three additional features capturing specific information about each vehicle: its fuel type (ICE, HEV, BEV), vehicle category (passenger, pickup, SUV, etc), and an identifier for each specific vehicle.

The decision to include all three of these additional features was not obvious; the vehicle ID is over-specific, and in a wider application would instead use a detailed model and trim-level specification. Furthermore, much of the predictive information in the vehicle’s fuel and category is shared with the vehicle ID, and as discussed in §2.2 mutual information and unnecessary features are to be avoided.

The core conflict is that on one side, some vehicle categories spanned a wide range of power levels (e.g., a modern F-150 base-model vs an older F-150 4x4 super-duty), best

addressed by permitting the model to modify power based on the observations of specific vehicles. On the other hand, some specific vehicles were only observed for a short period of time, and would not generalize well without reference to the information of other similar vehicles. On the balance, it was decided to include all three, since boosted tree models split on a single feature at a time, and therefore do not tend to overemphasize based on mutual information.

Once the feature-set was selected, the regression model's hyperparameters were tuned as described in §4.6.3, and power predictions made for each segment. The average per-segment MMAPE of this method matched that of the eigentrips model, at 32.3%.

# 5 Results

5.1	Presentation of Error . . . . .	58	5.3.1	Replacement by predicted distance . . . . .	66
5.1.1	Error measures . . . . .	58	5.3.2	Replacement by published fuel economy . . . . .	67
5.1.2	Chosen error measure . . . . .	60	5.3.3	Replacement by logged energy . . . . .	67
5.2	Discussion . . . . .	60	5.3.4	Replacement by best savings . . . . .	67
5.2.1	Error interpretation . . . . .	60	5.4	Shapley Additive Explanation . . . . .	68
5.2.2	BEV prediction . . . . .	62	5.4.1	SHAP overview . . . . .	68
5.2.3	PHEV prediction . . . . .	63	5.4.2	SHAP summary visualization . . . . .	69
5.2.4	HEV prediction . . . . .	63	5.4.3	SHAP implications . . . . .	70
5.2.5	Physical interpretation . . . . .	63			
5.3	Application . . . . .	65			

This section presents the predictive error of the proposed "eigentrips" model relative to the logger-data estimate of actual power. The eigentrips model is compared with two alternative means of prediction: first, business-as-usual prediction based on standard L/100km fuel economy figures, and second, an LGBM regression model trained to directly predict segment fuel consumption. The eigentrips model is piecewise-constant, so the regression model is presented to give a sense of the eigentrip model's avoidable quantization error.

Much of the discussion in this section is with regards to the MMAPE for individual 3-minute segments, since that is the most intuitive initial indicator of the model's accuracy. For the end user's purpose, trip-level or mission-level (ie, for the duration of the vehicle's participation in the study) aggregate error is likely to be of more interest, and that is addressed at greater length in the discussion section, §5.3.

## 5.1 Presentation of Error

### 5.1.1 Error measures

The most appropriate intuitive measure for prediction error was not immediately obvious, for the following reasons:

- Absolute (non-relative) error over-represents error in high-power vehicles.
- Relative (to actual-error) over-represents error when actual power is very low.
- Relative (to vehicle) requires a fixed per-vehicle denominator, resulting in unexpected error values for segments unrelated to the selected denominator.

Several measures of prediction error were considered, described below with their shortcomings. For the formulae below,  $a$ =actual,  $p$ =predicted,  $q$ =vehicle max power,  $\mu$ =vehicle mean power.

#### 1. MSE (mean squared error)

$$\epsilon = (a - p)^2 \tag{20}$$

Problem: Although  $Min(\Sigma MSE)$  is the model's actual objective function, it does not give a good intuitive grasp of the magnitude of the prediction error when actually applied to a real-world prediction problem. A lay user would expect that a model described as having 25% error will generate predictions incorrect by approximately 25%, not by 50%.

#### 2. $\eta$ (absolute/non-relative error)

$$\eta = |a - p| \tag{21}$$

Problem: Error will be exaggerated in high-power vehicles, and they will dominate summary results.

3.  $\epsilon_\mu$  (**relative to vehicle-mean**)

$$\epsilon_\mu = \left| \frac{a - p}{\mu_v} \right| \quad (22)$$

Problem: The mean can be different in similar vehicles, depending on operation. Some mission profiles are dominated by idle!

4.  $\epsilon_q$  (**relative to vehicle-max**)

$$\epsilon_q = \left| \frac{a - p}{q_v} \right| \quad (23)$$

Problem: Unintuitive at low power. EG: consider a 100kW vehicle, on a segment where actual power is 1kW and prediction was 2kW. This measure would return an error of  $\epsilon_q = (2 - 1)/100 = 1\%$ , even though the prediction was double the observed value.

5. **TMAPE (true mean absolute-value percent error)**

$$TMAPE = \left| \frac{a - p}{a} \right| \quad (24)$$

Problem: Segments with zero or near-zero actual power will have excessively high error. This is of particular concern with EVs and HEVs, which frequently "idle" at fractional kW power. Almost 1% of EV samples were observed at under 1kW, causing unreasonably high segment prediction errors.

6. **MMAPE (mean absolute-value percent error, modified)**

$$MMAPE = \left| \frac{a - p}{1 + |a|} \right| \quad (25)$$

This metric retains much of the intuitive power of TMAPE, while avoiding excessive error at for very small values of actual power.

Problem: The added 1 in the denominator is arbitrary. In the previous example,

Table 10: Error for various timescales, contrasting eigentrips model vs business-as-usual vs LightGBM regression

	L/100km (%)	Eigentrips (%)	Regression (%)
Segment	50.9	32.0	32.4
Trip	38.5	23.7	20.3
Mission	21.8	9.59	2.90
Study	19.3	7.45	0.120

Table 11: Per-trip error for various vehicle fuels/categories, contrasting eigentrips model vs business-as-usual vs LightGBM regression

Fuel	Category	L/100km (%)	Eigentrips (%)	Regression (%)
Electric	Passenger	47.8	64.8	127.
Gas	Cargo	43.9	56.0	34.1
	Pickup	51.6	35.1	21.0
	SUV	17.0	21.9	10.4
PHEV	SUV	34.6	38.9	33.5

$\text{MMAPE} = (2-1)/(1+1) = 50\%$ , which bears no contextual intuitive relationship to the error.

### 5.1.2 Chosen error measure

In the remainder of this chapter, modified MMAPE is used to compare and contrast relative error. The arbitrary 1 added to the denominator is a common means of addressing the near-zero error problem, while retaining a sensible range of relative error across the range of actual values.

## 5.2 Discussion

### 5.2.1 Error interpretation

Table 10 shows MMAPE at various levels of aggregation, split out for business-as-usual L/100km prediction, for the proposed eigentrips model, and for direct regression with the LightGBM comparison model. In general, the prediction performance is as

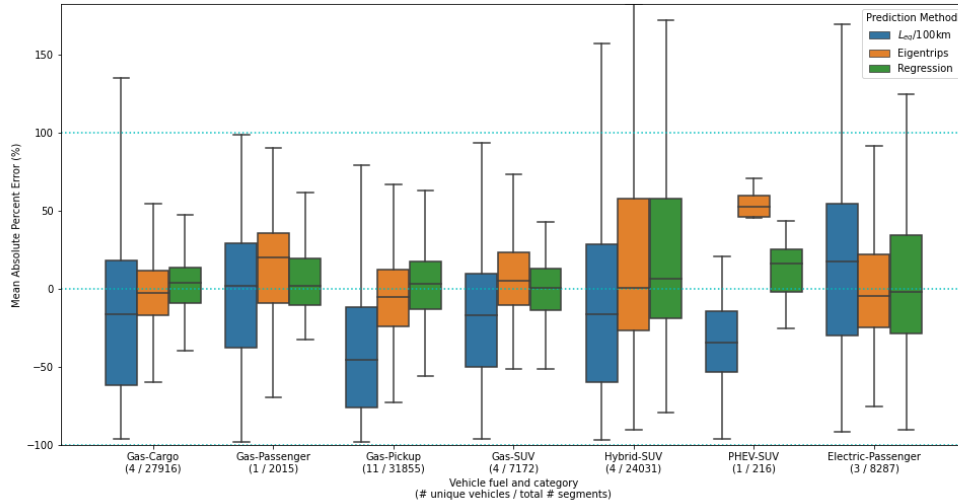


Figure 18: Prediction error distribution of segment-level predictions, contrasting eigentrips model vs business-as-usual vs LightGBM regression

expected: the eigentrips model outperforms traditional L/100km prediction, and is in turn outperformed by direct regression.

The segment level error for both the Eigentrips and Direct regression models is very high, and remarkably similar. Since the eigentrips model is expected to have significantly more error due to quantization inherent in the technique, the behaviour is anomalous, and suggests that the predictions are missing information relative to the ground truth. This may reflect an erratic ground truth (due to error in the MAF approximation of true fuel flow), or changes in power requirement disguised by missing features such as missing or inaccurate road grade, or other features discussed in §7.5.5.

Table 11 shows the per-trip aggregate error, broken down by "fuel" (actually drivetrain type) and vehicle category. It is noteworthy that the LightGBM regression model and eigentrips model did not perform particularly well for the various hybrid and battery-electric vehicles, although they did still tend to outperform traditional fuel economy.

Figure 18 shows the per-segment MMAPE for each fuel and vehicle type. The boxes show the quartile range of error values (25% and 75%, with a horizontal line to indicate median), with whiskers to show the extent of the 10th and 90th percentile. The plot does an excellent job of showing that in general, the LightGBM regression model and the eigentrips model have lower bias and lower variance than the L/100km technique.

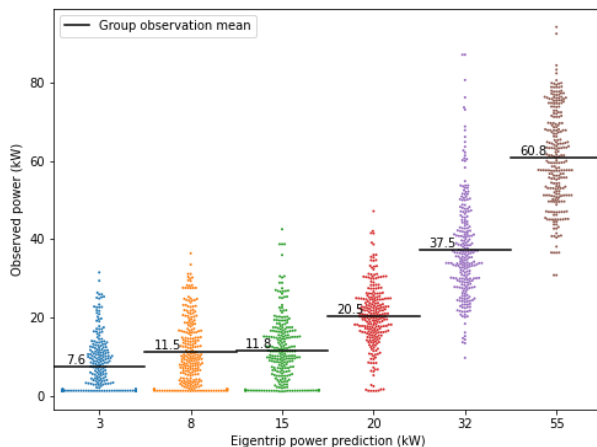


Figure 19: Example power versus prediction within eigentrips

However, this plot also shows unexpectedly wide variance for HEVs and BEVs, and high bias *and* variance for the PHEV, all discussed in detail below. It is also noteworthy that the  $L_e/100km$  prediction shows an error of -100% in many cases, since it has no means to appropriately predict idle power.

Figure 19 uses a single example vehicle to illustrate the variance in actual powers within each labelled eigentrip, presented in the form of a swarm plot against the power prediction, taken as the vehicle’s characteristic power. The horizontal bar on each swarm shows the mean *actual* power, which is seen to be quite close to the quantized *predicted* power – which is the vehicle’s characteristic power for that eigentrip.

### 5.2.2 BEV prediction

For the BEVs, this excessive variability is attributed largely to the 90-second low-resolution power sampling discussed in §3.3. Although the BEVs’ onboard SOC computation is presumed to be reliable, it is impossible to know how much power consumption is measured in one segment when it is better attributed to the next. This lack of accuracy is a key outcome of this research: high-resolution data-driven energy prediction requires high-resolution input data.

It is noteworthy that since the reported error is relative to actual consumption, the apparent error of the BEVs is amplified relative to the ICEVs; the 25-75 IQR in figure

18 shows that the eigentrip model has about double the relative error for BEVs as for ICE pickup trucks – but since the BEV’s power is so much lower, this in fact represents a prediction of  $35.7 \pm 7.0$  kW for the pickup truck, and  $3.0 \pm 0.88$  kW for the BEV; the BEV’s absolute error range is in fact much smaller.

### 5.2.3 PHEV prediction

The single PHEV suffered from the same low-resolution sampling problem as the BEVs, and additionally had a very short data-collection period, with only 216 travel segments recorded, totalling about 10 hours of travel.

Furthermore, the PHEV had no mechanism for capturing the likelihood that a given segment is in ICE-mode. Future work with PHEVs should attempt to create additional kinetic features to capture that information, such as total distance travelled this trip, or total distance today.

### 5.2.4 HEV prediction

The study included 4 Toyota RAV4 mild HEVs, which were predicted with a reasonable MMAPE, but a wide spread in the segment level predictions. The loggers in the HEVs were not configured to capture HV battery status, so it can be presumed that the short-term error included a significant amount of energy consumption being shifted between adjacent segments, EG, by regenerative braking.

Improving HEV energy prediction would be an interesting extension to this work, and would require additional feature engineering to capture HEV-specific behaviour, such as regenerative braking and any periods of sub-optimal engine operation.

### 5.2.5 Physical interpretation

Figure 20 shows a box plot for each kinetic feature, showing the distribution of values broken down by eigentrip label. Examination of these plots may help with understand-

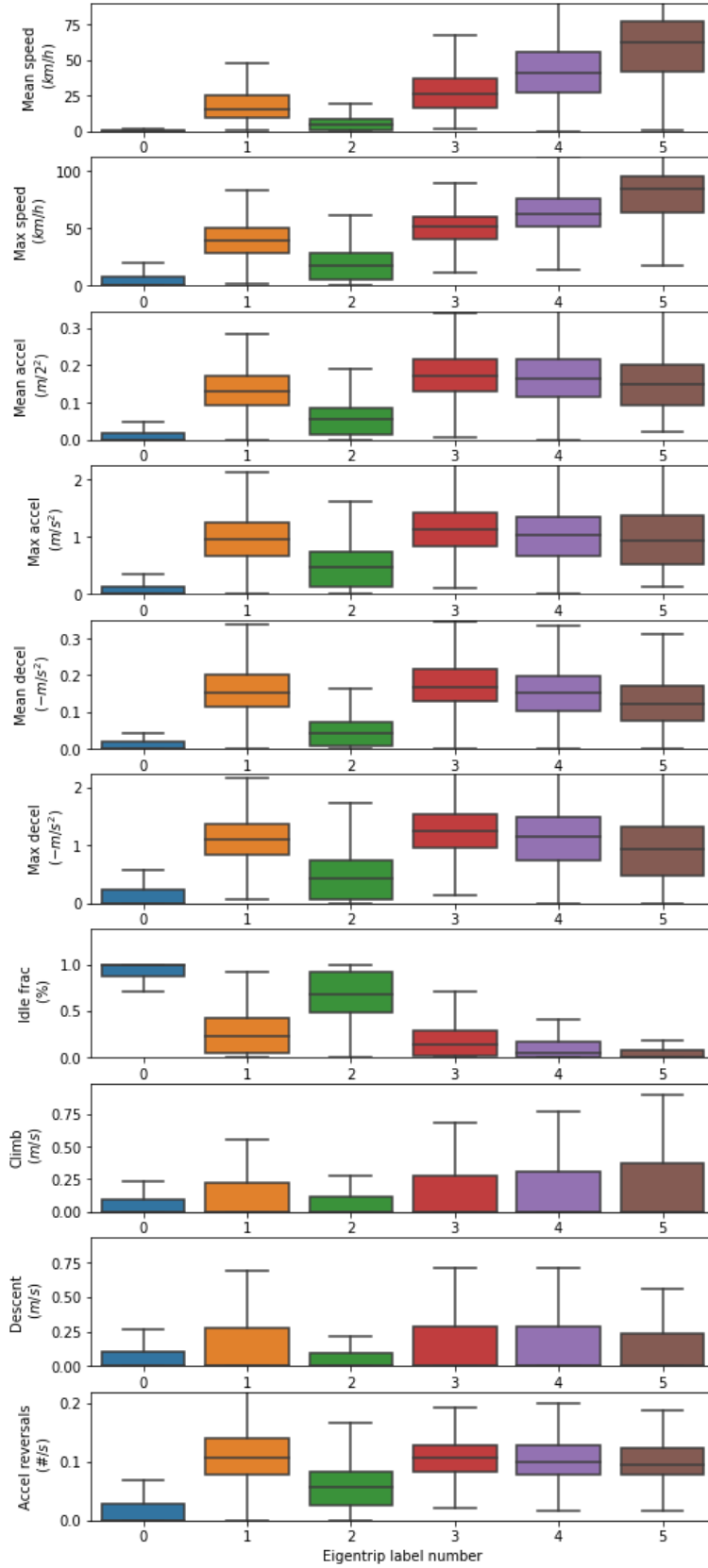


Figure 20: Per-eigtrip distribution of feature values across all missions

ing of the physical nature of travel likely to be labelled as most similar to a particular eigentrip.

### 5.3 Application

To illustrate the application of the eigentrip model, imagine that a fleet manager has been allocated budget for three new vehicles, with the explicit goal of minimizing annual carbon-based fuel consumption. The manager is faced with the decision of which vehicles to replace. Without logger information (and, for this purpose, in the absence of mission constraints) the decision will be informed by whatever information is at hand.

This section explores the information that the manager might have, the vehicle replacement decisions they might make with various information, and the likely impact of those decisions in light of the logger data. The impact is given in terms of saved energy in MJ, and the volume of consumed gasoline for ICEVs. Additionally, to highlight the impact of high-efficiency BEVs consuming low-intensity BC grid electricity, the related GHG emissions are also listed, given global warming potentials (GWPs) of  $88.1 \text{ g } CO_2_e/MJ$  for gasoline [9] and  $2.96 \text{ g } CO_2_e/MJ$  for BC Hydro’s grid electricity [10].

Fuel consumption in this section is given relative to a power baseline derived from the logger MAF and SOC data, as described in §3.3. As discussed in §7.5.2, the validity of this baseline estimate is one of the study’s core assumptions – there is no validated fuelling data from which to calculate error bars.

The prediction estimates are given as maximum likelihood values – given the vehicle’s single characteristic power value for each eigentrip, and a count of the most-probable eigentrips for the mission, the prediction estimate becomes a simple dot product. As discussed in §7.3.6, it would be valuable to have a generalized measure of uncertainty for each mission-vehicle prediction, but this would require characterizing each mission and vehicle as a probability distribution rather than a singular value, defeating the model’s core goal of simplicity. To give *some* sense of the prediction reliability and impact on decision-making, the replacement vehicle’s whole-study MMAPE is applied

Table 12: Whole-mission error averaged for various vehicle fuels/categories, contrasting eigentrips model vs business-as-usual vs LightGBM regression

FuelType	L/100km (%)	Eigentrips (%)	Regression (%)
Electric-Passenger	20.7	15.3	19.2
Gas-Cargo	20.1	13.8	9.43
Gas-Pickup	40.2	9.55	11.2
Gas-SUV	9.44	7.15	0.685
PHEV-SUV	40.2	0.0965	2.85

to the resulting prediction. The replacement vehicle in all cases happens to be the Kia Soul BEV, so an expected error of 10.7% is selected from the Electric-Passenger row of table 12 and calculated for each prediction.

### 5.3.1 Replacement by predicted distance

If the fleet manager has accurate mileage records and can predict the mission distances, then they might choose to predict per-mission energy consumption by multiplying predicted mission distance by the published fuel economy of the vehicle currently assigned. The top three energy consumers by this prediction would be two pickup trucks and a van, predicted to annually drive 58,700 km, and to consume 246 GJ of fuel.

The actual logged consumption of these three vehicles extrapolated to a full year was in fact 350 GJ (equating to 10300 L of gasoline, and GHG emissions of 30900  $kg CO_2e$ ) – an error of 24%, illustrating that this method is not particularly accurate. Applying the eigentrips model, we find that replacing these three vehicles with a BEV similar to one of the tested passenger vehicles (not actually an appropriate replacement for a cargo vehicle) would result in a predicted consumption of 26.9 GJ, and cause GHG emissions equating to about 79.7  $kg CO_2e$ . This replacement, if it were possible, would save 321 GJ of energy and avoid 30800  $kg CO_2e$  of GHG emissions. The expected prediction error of 10.7% for this vehicle category equates to an error estimate of  $\pm 2.88$  GJ and  $\pm 8.5$   $kg CO_2e$ .

### 5.3.2 Replacement by published fuel economy

Lacking mileage or fuelling records, the fleet manager might select the three vehicles in the fleet with the worst fuel economy ratings – two pickup trucks and an SUV, in this example. In the absence of distance or fuelling records, there will be no predicted consumption better than the manager’s educated guess, perhaps by pro-rating the fuel budget for the entire studied fleet (1167 GJ) by fuel economy numbers, resulting in a predicted consumption of 203 GJ.

The extrapolated logger data suggests that these vehicles would have a total annual consumption of 200 GJ (5900 L gasoline, emitting 17600 *kg CO<sub>2e</sub>* of GHGs). Their BEV replacements would result in a new predicted consumption of 14.9 GJ (44.2 *kg CO<sub>2e</sub>*) – a savings of 185 GJ, and avoiding 17600 *kg CO<sub>2e</sub>* of GHG emissions. The expected error of 10.7% equates to an error estimate of  $\pm 1.60$  GJ and  $\pm 4.73$  *kg CO<sub>2e</sub>*.

### 5.3.3 Replacement by logged energy

In the absence of actual pump-to-tank records, the loggers themselves have the best record of the energy consumed by each vehicle. Extrapolating each vehicle’s actual logged consumption to a year, the top three consumers will total 388 GJ (11500 litres gasoline, emitting 34200 *kg CO<sub>2e</sub>*). Their BEV replacements would consume 25.7 GJ (76.3 *kg CO<sub>2e</sub>*), saving 362 GJ and avoiding 34100 *kg CO<sub>2e</sub>* of GHG emissions. The BEV’s expected error of 10.7% equates to an error estimate of  $\pm 2.75$  GJ and  $\pm 8.16$  *kg CO<sub>2e</sub>*.

### 5.3.4 Replacement by best savings

The theoretical best solution is to consider all missions, and select the replacements offering the highest predicted savings over the incumbent vehicles. In this case, the result happens to be the same as the case above: replacing the highest energy consumers with the most efficient available alternative. However, this would not be the case if the highest energy consumers were already relatively efficient.

Table 13: Illustration of SHAP for a single prediction

	Feature Values	SHAP Values
Speed	52.8	18.8
Max speed	64.7	1.01
Acceleration	0.125	-0.382
Max acceleration	1.03	0.0332
Deceleration	0.104	0.797
Max deceleration	1.06	0.195
Idle	0	-0.769
Climb	0.324	0.0151
Descent	0.273	-3.32
Acceleration reversals	0.15	1.85
vid	Vehicle 10	23.1
Type	Pickup	4.8
Fuel	Gas	2.16

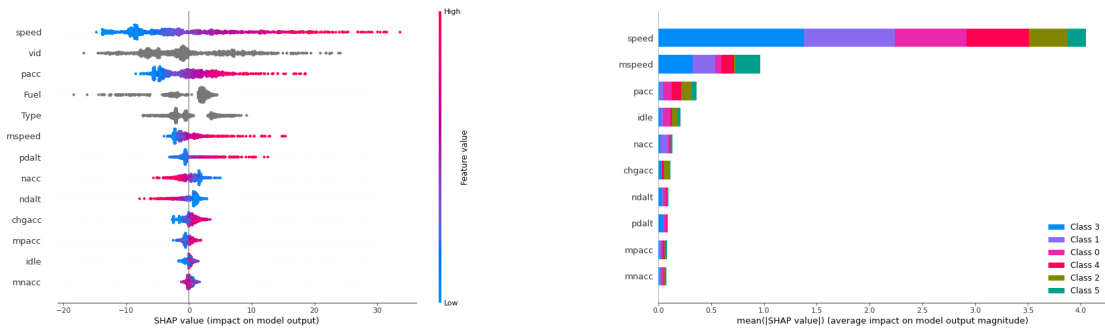
## 5.4 Shapley Additive Explanation

### 5.4.1 SHAP overview

Shapley additive explanation (SHAP) [71] is a method for understanding the contribution of each individual feature to a specific final prediction. The explanation is *additive*, because the individual contributions sum to the actual prediction.

To illustrate, consider the lightGBM regression comparison model described above in §5.2, applied to predict the power of a single segment vector. An example is shown in the "Feature Values" column of table 13. The SHAP explainer constructs a general null prediction (an estimate in the absence of any feature information, typically the training mean), and then computes the individual additive contributions of each feature to increase or decrease the specific prediction under consideration from the general null prediction. In this case, the sum of the 28.4 kW null prediction and the individual SHAP values (again, shown in table 13) is equal to the regression model's final prediction of 89.0 kW.

The method of computing the individual feature contributions is somewhat involved. Mazzantzi has written an excellent simplified explanation in [72]. Further summarized, the method involves creating a directed graph of models for every possible combination



(a) Regression SHAP, showing feature relationship to prediction impact (b) Multiclass SHAP, showing absolute feature impact on individual class membership probabilities

Figure 21: SHAP explanation summaries, showing each feature’s contributions to the model’s prediction, across the entire dataset

of available features, arranged such that the edges in the graph imply the addition of an individual feature relative to the source node. The contribution of a feature is a weighted average of the change in predicted values along all the edges where that feature is added.

### 5.4.2 SHAP summary visualization

A second application of SHAP is to explain the relative importances of the features, across all samples in a dataset [73]. It is easy to imagine, for example, that the climb rate feature would have a much larger impact on the visible power requirement of a heavily loaded ICE cargo vehicle, as opposed to a mild hybrid using its traction battery to invisibly average its engine power output between climbs and descents.

Figure 21(a) addresses this requirement by showing the distribution of absolute contributions of each feature to the predictions. For numeric values, red implies a high value, and the right side of the chart indicates a positive impact on the power prediction. EG, higher mean speed (red) tends to increase the power prediction (i.e., rightward), and a low mean speed (blue) tends to decrease the power prediction (i.e., leftward). The categorical features have no scalar values (grey), and this SHAP visualization has no intuitive way to show *which* categories shift the prediction in a particular direction; the only information presented is the range of impact magnitudes caused by various values

in the feature.

The eigentrip technique centrally uses a multiclass classifier, not a regression model; the classifier’s output for each prediction is in fact a vector of class probabilities, rather than a single predicted value. Plot (a) could at best be used to show the absolute impact of each feature on the probability of predicting one of six eigentrips. Instead, figure 21(b) illustrates the *mean absolute* impact of each feature on each class probability – in other words the absolute change on the prediction probability if the feature is known, vs not known. For example, the figure shows that knowing the Speed value tends to change the probability of class 3 by an absolute magnitude of about 1.4; it has a large impact, although the plot gives no information about whether the impact tends to be positive, negative, or even mixed.

### 5.4.3 SHAP implications

On the summary figure(21a), the features for acceleration reversals (chgacc), maximum positive acceleration (mpacc), idle fraction (idle), and maximum deceleration (mnacc) are seen to have relatively small contributions to the prediction.

To illustrate that this is valid, the regression and eigentrip models were re-applied with reference to only the *other* features. The impact of deleting these less-important features from the direct regression model was indeed quite modest, increasing the average segment MMAPE by only 0.21% – from 32.7% to 32.9%.

The impact on the Eigentrips model was somewhat more significant, increasing from 32.1% to 39.4% – perhaps highlighting the impact of an increased number of marginal samples no longer being nudged into the correct classification by the additional features.

## 6 Conclusions

The eigentrip approach developed in this research has reasonably good accuracy, and produces whole-year mission predictions averaging a MAPE of 9.4%. The concept can be expected in the field to give significantly better predictive results than the baseline (L/100km) method's MAPE of 22%, although there is clearly room for improvement, as shown by the direct-regression model's average MAPE of 3.7%.

The reduced error of either machine-learning model is balanced against added complexity; adding a new vehicle to the model would require computing the new vehicle's per-eigentrip characteristic power values. Similarly, adding a new mission profile (or updating a modified one) would require logging some weeks worth of representative travel data, sanitizing it, and deconstructing it into a combination of eigentrips.

The criterion of spreadsheet-compatibility no longer seems as important as it originally was, due to the advent of low-barrier options for deploying ML models in the cloud, such as managed notebook hosting services. Such a model would have better predictive accuracy, and could be designed to facilitate the direct upload of new data – either representing new vehicles, or in order to better represent the evolution of the fleet's mission profiles. That said, a spreadsheet-deployed model would still be helpful to address potential concerns around the public exposure of individual travel information. This issue was deeply significant for the CRD, whose requirements informed this research.

The research performed here has been severely limited on several fronts, hampered by data collection problems and limited by inadequate temporal resolution. One of the initial goals, choosing the best of several alternative high-efficiency replacements, has been rendered impossible by the elimination of alternatives in the source data – the initial study was intended to include several HFCEVs, PHEVs, and other types of BEV beyond the Kia Soul EV. None of the desired alternatives were ultimately included in the logged data, and the single PHEV logged only about 10 hours of travel time before the data collection phase was terminated.

An important outcome of this research is reinforcement of the idea that any data-driven

model for predicting per-trip or per-mission vehicle energy consumption will be limited in accuracy by the quality of the data that informs it. A good model would require higher-resolution input data, and an exploratory data campaign facilitating iterations of the experiment with various sampling frequencies and methods would be yet another excellent subject for further study.

Ultimately, a data-driven model will be an effective recommendation tool for selecting replacement vehicles to minimize energy consumption and carbon footprint. Careful design of a data collection strategy will be the foundation of any trustworthy model.

# 7 Recommendations and Future Work

7.1 Assumptions . . . . .	73	7.4 Modeling . . . . .	81
7.1.1 Stationarity and ergodicity	73	7.4.1 Improved clustering . . . . .	81
7.1.2 Baseline energy consumption . . . . .	74	7.4.2 Probabilistic class membership . . . . .	82
7.1.3 Standardized GHG intensity	75	7.4.3 Prediction error and missing features . . . . .	82
7.1.4 Fixed MAF ratio . . . . .	75	7.4.4 Characteristic power by vehicle model . . . . .	83
7.1.5 Clustered eigentrip definitions . . . . .	76	7.5 Data and Features . . . . .	83
7.2 Cleaning Decisions . . . . .	76	7.5.1 Data requirements . . . . .	83
7.2.1 Smoothing starts . . . . .	77	7.5.2 High-quality energy input data . . . . .	83
7.2.2 Regularization . . . . .	78	7.5.3 Road grade . . . . .	84
7.2.3 BEV power interpolation . . . . .	78	7.5.4 Features to support other vehicle types . . . . .	85
7.3 Data Structure . . . . .	78	7.5.5 Other features . . . . .	85
7.3.1 Time-domain features . . . . .	78	7.6 Applications . . . . .	86
7.3.2 Feature evaluation . . . . .	79	7.6.1 Real-time allocation . . . . .	86
7.3.3 Microtrip boundaries . . . . .	79	7.6.2 Information sharing . . . . .	86
7.3.4 Clock time segment boundaries . . . . .	79	7.6.3 Connected Vehicles . . . . .	87
7.3.5 Iterative segment refinement	80		
7.3.6 Characterize as distributions	80		

This section discusses a number of limitations, assumptions, and other potential improvements to the studied process and model.

## 7.1 Assumptions

Several simplifying assumptions were made that could benefit from more rigorous treatment, either to quantify the resultant error, or to find a more precise method.

### 7.1.1 Stationarity and ergodicity

This entire study is predicated on two key assumptions: that the power and kinetic features are stationary (i.e., that the statistics do not change over time) and that they

are ergodic (the statistics do not change erratically and inconsistently with respect to uncontrolled parameters).

All of this is to say that the work assumes that the kinetic features are dictated by the mission, and not unduly influenced by changing factors such as the physical characteristics of the vehicle, the habits of the driver, and changing traffic patterns. Future work should validate and quantify these assumptions by observing the same mission operated with different vehicles, and confirming that e.g., a difference in power or handling characteristics doesn't result in a confounding change in the observable kinetic features.

Most power-impacting differences in driver habits would likely be captured and accounted for in the speed and acceleration features. However, an exploration of driver-mission and driver-vehicle stability might be warranted since (a) drivers might affect non-engine power consumption, such as climate control, changing the power characterization of a vehicle, and (b) a difference in driving technique might be so extreme as to alter the kinetic profile of a measured mission, depending on who is driving it.

The same assumptions apply to the per-vehicle characteristic power values. Future work should compare data collected from similar or identical vehicles, while driven by different drivers, in different missions, in different geography, and in different organizations.

### **7.1.2 Baseline energy consumption**

This thesis evaluates the validity of the new method for predicting energy consumption, as compared to the traditional model-specific fuel economy statistic measured in  $L_e/100km$ . The validity of the two predictions is compared by measuring error relative to the best available estimate of "actual" energy consumption, as derived from MAF and SOC.

It is a significant assumption that the inferred estimate of input energy from logger values is valid and correct. As discussed in §7.5.2, it would be a significant improvement to this research to collect actual per-vehicle fuelling records for ICEVs and electrical

metering for grid-powered BEVs in order to establish the accuracy of the logged energy consumption estimates.

### 7.1.3 Standardized GHG intensity

A primary intended use of this work – the prediction of GHG emissions – presumes that it is possible to easily convert a known quantity of input energy into a specific GHG footprint in kg CO<sub>2e</sub>, by applying standard GHG intensities such as those published by the BC Canadian Ministry of Environment & Climate Change Strategy (MOE) or BC Hydro [74, 10].

Events such as Volkswagen's "Dieselgate" [75] have made it clear that this is a weak assumption for ICE vehicles, and that there may be a need for model-specific intensity factors. Further investigation will be necessary to quantify the associated error.

Other factors may impact the emissions calculation for grid-powered BEVs, depending on how grid emissions intensity is to be calculated. BC Hydro reports an overall carbon intensity of 11  $gCO_2e/kWh$ , with specific renewable and fossil sources rated at 4g and 593g respectively, and conducts a significant bidirectional trade with Alberta, which is attributed an intensity of 820g [76]. A 2017 paper found that carbon intensity in New Zealand should be considered as varying between 32g and 188g depending strictly on time-of-day [77]. It is easy to imagine a dynamic fleet model with reallocated vehicles according to changing requirements for calculating emissions, or even from the time-dependent change in the carbon intensity attributed to their power sources.

### 7.1.4 Fixed MAF ratio

Fuel consumption rates were inferred from the OBD2 log values for MAF. This is only accurate if the fuel:air mixture is known. The stoichiometric ratio of 14.7 is commonly accepted [54], and as described above in §2.3.2, the author's undocumented personal experience supports it. No peer-reviewed literature nor authoritative texts were found supporting or refuting this assumption.

Since fuel flow is not a standard OBD2 PID, it would be an excellent contribution to the literature to publish a model or a dataset helping to more accurately infer actual fuel flow from MAF and other standard OBD2 parameters.

### 7.1.5 Clustered eigentrip definitions

An early assumption was that the eigentrip definitions should be inferred from the data, rather than synthesized from expert knowledge of how different driving patterns are likely to influence fuel consumption. The basis set was therefore constructed using unsupervised clustering.

It would be possible to instead construct a set of exemplar trips that are representative of trip-types which a domain expert intuitively believes are likely to be predictive of energy consumption variability between vehicle types. Examples might include situations such as

- point-to-point highway travel, off-peak hours
- highway travel, rush-hour
- point-to-point city travel
- patrolling and parking enforcement
- idling to supply vehicle-mounted equipment

If the eigentrips were modelled on intuitively understandable travel-type exemplars, users would be better able to infer the nature of new or blended missions, and be better able to apply sanity checking to unexpected model results.

It would be interesting to repeat the experiment with such a set of intuitive eigentrips, and contrast the level of error with that found from the inferred ones.

## 7.2 Cleaning Decisions

The extensive data cleaning and preparation process required a number of judgement calls and simplifications. The most important of those are listed here.

### 7.2.1 Smoothing starts

As discussed above in §3.2.3, a large number of in-motion samples immediately following an at-rest sample were dropped due to impossibly high accelerations, presumably due to sampling errors.

Simple rejection of these potentially informative samples was to be avoided. An aborted attempt was made to impute reasonable speed profiles to these samples using the following process:

1. Compute a “typical low-speed acceleration” for each vehicle, consisting of the median of in-motion positive acceleration values at speeds below an arbitrary threshold of 15 km/h.
2. For vehicle starts with impossibly high logged accelerations, the zero-speed sample is time-shifted to an earlier time that would reflect that vehicle’s typical acceleration – but never such that it would precede the prior speed sample.
3. If the time-shifting would cause the zero-speed sample to precede a legitimate logged non-speed sample, then “required acceleration” is computed from that legitimate sample. If that required acceleration is found to have a reasonable magnitude, then the earlier sample time is retained and deemed to be the new start time.

Unfortunately, many of the error periods were found to bracket other sensor readings, particularly MAF readings. Inserting an imputed speed value would call into question the validity of the the subsequent MAF observation, causing irreconcilable discrepancies between inferred acceleration and inferred fuel flow. The method has potential, but requires detailed review of the original datastream to be sure that it was not introducing more error than it is removing.

### 7.2.2 Regularization

As discussed in §3.4, the entire corpus was regularized to 1s intervals to simplify segmentation. This implies linear interpolation and extrapolation – both of which unavoidably introduce error relative to the actually-measured real samples.

Given the potential to process variable-length segments as discussed in §7.3.5, it would instead be possible to divide segments precisely at sample times, minimizing the amount of interpolation required.

### 7.2.3 BEV power interpolation

Since sampling of the BEV’s power was done at a relatively low resolution, a simple time-interpolation on SOC was performed to help estimate power consumption within each trip segment.

Hopefully future work will have direct access to higher resolution BEV power data.

With only the data at hand, a number of techniques might do better at predicting SOC at the segment boundaries, perhaps using a timeseries regression model inferring from additional other features such as distance travelled and acceleration profile.

## 7.3 Data Structure

### 7.3.1 Time-domain features

As discussed in §2.2.2, there are good reasons for this model to be structured as a non-timeseries problem. However, there are likely to be some time-domain or frequency-domain features with predictive power. Examples for possible exploration include the effects of stop-and-go traffic and time-of-day. Possibilities to extract predictive features from these characteristics include spectral power density [42] as a fingerprint feature, and the use of time-domain techniques like Kalman filters, [78] might help to generate predictions of otherwise unknowable state features such as the vehicle’s kinetic energy

or a mild hybrid's drive battery SOC. Another possibility is the employment of dynamic time warping, [79] or wavelet convolutions [80] in order to find recurrences of observed patterns that might characterize driving segments as being similar.

### 7.3.2 Feature evaluation

The initial short set of features in §4.1 is based on the work of others [38]. It would be a valuable contribution to compile an exhaustive list of features directly available from OBD2 or computed from them, and apply a rigorous evaluation for relative predictive power. A simple example is the selection of the 98th percentile to illustrate the feature "maximum acceleration". It is possible that some other quantile (or even the unfiltered maximum observed value) would be more predictive.

One method for this would be to derive an expanded feature set (such as those listed in §2.1.2), and apply SHAP [73] analysis to determine which features are most predictive of energy consumption.

### 7.3.3 Microtrip boundaries

An early assumption was the rejection of stop-go-stop microtrips as the fundamental trip segment, due to concern about excessive mixing of trip types. The requirement for fixed-length segments added significant complexity to the data preparation phase.

It is possible that the presumptive concern is unfounded. It would be interesting to perform the entire experiment again with microtrips to see the impact on prediction accuracy.

### 7.3.4 Clock time segment boundaries

For simplicity, the segments were regularized to clock time, beginning at even multiples of three minutes from 00:00:00 each day. This assumption results in final and initial segment in each trip being shorter by an average of 50%. Since each segment is given equal weight in the model, this difference over-weights the importance of measurements

in those segments. However, since the first and last segments might legitimately have more predictive power than mid-trip segments, it is possible that over-weighting them is doing more good than harm.

It would be reasonable to validate this assumption by using only segments of precisely 3 minutes' length, discarding a contiguous period of "leftover" modulus samples between a random segment-pair.

### **7.3.5 Iterative segment refinement**

Another simplifying assumption was the use of segments of specified (3-minute) constant duration. This naturally has the following effects at the arbitrary boundaries:

- combines disparate travel types into single segments
- arbitrarily splits similar travel types, creating unneeded additional segments

A refinement to this approach would be to use the boundaries defined by the initial classifier in order to re-partition the travel data. Given an initial set of characteristic travel types, it would instead be possible to segment the trip at "type boundaries", where travel transitions from one type to another. This would result in segments of variable length, but of more consistent travel types. It is to be expected that this would result in more accurate energy consumption prediction within each travel type.

### **7.3.6 Characterize as distributions**

The eigentrips model characterizes each vehicle as a vector of characteristic power values for each eigentrip, and each mission as a vector containing the sum of time spent in each eigentrip. The prediction of energy for applying a vehicle to a new mission is the dot product of the two vectors. This value does not give any reflection of the prediction's level of uncertainty, and it would be preferable to have some sense of the variance of the prediction.

Many regression models (including LightGBM) support so-called "quantile regression", allowing the model to output a prediction interval – eg, the 90th percentile model will

return a prediction indicating a value higher than 90% of actual expected values. This allows the user to intuitively understand the broadness of the prediction, as well as its central value.

This intuitive simplicity does not transfer to the eigentrips model. Extracting the 90th percentile energy prediction from a combination of vehicles and missions is *not* the dot product of the 90th percentile characteristic powers with the vector of singular mission times. It would instead require the computing the product of the nonparametric random variable representing the distribution of characteristic powers, with the eigentrip class probabilities, and determining the desired interval limits of the resulting product distribution.

Given that a primary goal of the eigentrips model is simplicity, this is *not* a recommended topic for future research. If a prediction interval is required, direct quantile regression would be a simpler and more reliable path.

## 7.4 Modeling

### 7.4.1 Improved clustering

The clustering step was performed by means of the well-known K-means algorithm, which returned a set of cluster centroids that were effective and useful, and which provided an excellent basis to prove the concept. The number of clusters was selected by inspection (the "elbow method"), and it would be informative to investigate more refined methods.

Other clustering mechanisms which do not presume spherical, normally distributed data would be likely to provide more representative centroids, and/or would lead more directly to an optimal number of clusters. For example, density clustering is a well-regarded process when the appropriate number of clusters is not known, however it was deemed unsuitable since the dataset is continuous without sparse regions between clusters.

Finally, the simple method used to select centroids predictive of energy consumption (adding weight to the energy consumption feature) does not necessarily select the optimal centroids for the following criteria:

1. minimize error from the selected fuel consumption model, but
2. are maximally discriminatory on fuel consumption for at least some vehicle features
3. provide adequate representation for all vehicle-eigentrip pairs

Finding centroids that meet all of these criteria may require developing a clustering strategy from first principles. A good first step would be to implement a GMM clusterer from first principles, in such a way as to allow feature-weighting.

#### **7.4.2 Probabilistic class membership**

Multiclass classifiers initially provide a probability of membership in *every* class, and only provide a singular prediction by application of maximum likelihood. A preliminary experiment with pro-rating segment time to \*all\* eigentrips by class probability was found to increase segment MAPE by nearly 50%.

However, for segments which fall close to the boundary between two (or more) segments, it seems reasonable that the segment's power contribution is likely to fall somewhere between the characteristic powers of the nearest segments. It might therefore be reasonable to assign the segment a blended contribution to energy consumption, weighted by the fractional probability of its nearest eigentrips. Since there is no requirement that a travel segment be characterized by whole numbers of eigentrips, it would be entirely acceptable to use multiple fractional membership, if it were found to reduce error.

#### **7.4.3 Prediction error and missing features**

Evaluating the actual operation associated with clusters that have the highest predictive error will be an excellent starting point for determining whether additional features are

needed to improve accuracy.

#### 7.4.4 Characteristic power by vehicle model

Predictions are executed by multiplying the number of eigentrips by the characteristic eigentrip power as calculated for each individual vehicle. It would be valuable to have an understanding of the model's accuracy when energy consumption is predicted by vehicle *model or category*, rather than by specific vehicle. Figure 17 shows the spread of characteristic power values within each vehicle category in the study. It appears that each category's power is relatively consistent, in spite of each category containing several models with different performance characteristics.

## 7.5 Data and Features

### 7.5.1 Data requirements

This model has been demonstrated to generalize quite well, even when trained on only 10% of the available data. An interesting exploration would be to evaluate how much log data is required to accurately characterize each mission profile.

Additionally, when a new vehicle type is added to the fleet, it would be valuable to know how much logging (and of what sorts of travel) should be conducted before its power consumption characteristics are sufficiently well known for use with this model.

### 7.5.2 High-quality energy input data

As described in sections 2.3.2 and 3.3, the fuel and electrical consumption data logged for this project was not of ideal quality. It would be an excellent extension to this work to evaluate its accuracy against target energy data of known accuracy. To that end, future work would be well-served by a logger-data corpus that includes:

- time-integrated fuel-flow (IE, total fuel since last sample) OR
- fuel-flow sampled at 1s resolution or better, OR

- all PIDs necessary to accurately calculate fuel flow, such as MAF and commanded air-fuel equivalence ratio

Additionally, in fleets where vehicle fuelling is controlled and monitored through a per-vehicle card system, it would be instructive to cross-check logger consumed-fuel totals against actual pumped-fuel totals.

For EVs, charging totals could be compared to consumption totals to evaluate accuracy and charge-discharge efficiency.

### 7.5.3 Road grade

Road grade has an obvious impact on power requirements, and can be expected to illustrate a significant difference in energy consumption between conventional vs hybrid or electric vehicles. A reliable road-grade feature would be an excellent addition to this study.

Positive and negative vertical speed features were calculated from the available GPS data. Unfortunately, the altitude feature was completely missing from a significant fraction of travel data. The feature was informative, improving predictive error from 45% to 35% in spite of large gaps in coverage, and the inherently low precision of the GPS altitude signal.

Since the horizontal accuracy of GPS is better than vertical, consideration was given to the idea of extracting elevation data from an open elevation dataset, such as NRCan's High Resolution Digital Elevation Model [81], based on the vehicle's reported coordinates. A preliminary investigation of this technique showed improvement, but still yielded an unfortunately high fraction of impossible grades, perhaps due to a failure of the terrain dataset to account for the significant amount of grade smoothing involved in road building in the Victoria area. This method showed some potential, but was felt to be a large source of complexity for an unknown amount of predictive power; it may merit future study, but is neglected in this work.

The best realistic source for road grade would be a barometric altimeter. For example,

The Freematics open-hardware logger provides for the direct integration of external sensors [82]. It would also be an interesting side project to determine whether the OBD2 PID 0x133 (barometric pressure) [83] has sufficient precision to be used for a road grade calculation.

#### 7.5.4 Features to support other vehicle types

Prediction was less precise than anticipated for the high-tech, high-efficiency vehicles. In particular:

- Prediction was poor for the mild HEVs. Investigation will be required to determine what additional features are required to capture hybrid performance, such as HV battery state, or additional kinetic features related to stop-and-go behaviour that could be impacted by regenerative braking.
- The BEV had a very wide range of error. Higher-resolution power data will be required, but they might also benefit from additional features indicating stop-and-go performance.
- If multi-fuel vehicles become common, a kinetic feature will be needed that can differentiate the circumstances under which they will switch from one energy source to the other. EG, total travel distance this day, or since last charge would probably work well for PHEVs.

#### 7.5.5 Other features

There are other known/predictable factors that might be suspected to have a significant impact on fuel consumption, although most of them would present substantial data-collection challenges. Examples include:

- payload, particularly in heavy vehicles. It could be estimated given road grade and high-resolution torque and acceleration.
- different drivers, subject to privacy concerns
- accessory load

- environmental load
- vehicle maintenance status
- road type, perhaps inferred from GIS data
- traffic density by location and time-of-day, perhaps from a data source such as Google Maps
- rigorous collection of vehicle sub-model and trim level

## 7.6 Applications

The originally envisioned application was evaluating re-allocation of existing vehicles, and evaluating procurement decisions for additional copies of existing known fleet vehicles. This subsection addresses additional potential applications.

### 7.6.1 Real-time allocation

It would be reasonable for a booking system to respond to a request for a pool-vehicle by preferentially assigning the vehicle which is most energy-efficient (or most GHG-efficient) for the specific task at hand. The proposed system is simple enough to be implemented in a browser-based booking application, allowing the back-end to be simplified to a simple database lookup for availability, potentially requiring no additional custom back-end software development.

### 7.6.2 Information sharing

If multiple municipalities (or other organizations) established a shared set of eigentrip definitions, it would allow them to share information about their vehicles and their missions.

Vehicle information sharing would allow organization A to evaluate the local performance of a vehicle model owned by organization B.

On the other hand, sharing mission information sharing might highlight opportunities to improve operational efficiency. For example, organization A's parking enforcement

mission might have a much more efficient eigentrip profile, as its new optical license plate reading equipment allows it to spend a much higher portion of its time cruising rather than idling. The improved energy performance might be sufficiently impressive to encourage organization B to acquire the same equipment, solely to save the associated vehicle emissions.

### **7.6.3 Connected Vehicles**

The advent of fully-connected vehicles (e.g., Tesla and other new EV manufacturers) has potential to provide a ready source of detailed, high-resolution vehicle performance data. It would be quite simple for a manufacturer to publish real-world samples of operations logs, allowing potential buyers to evaluate mission-vehicle energy and GHG performance without any need to purchase an evaluation copy.

It would also be reasonable to establish a universal set of eigentrips, allowing manufacturers to publish statistically verifiable real-world performance statistics for their vehicles.

Having new vehicles providing logger information by default would provide other opportunities when connected to a power-vs-mission analysis. For example, departure from manufacturer-published vehicle performance statistics could trigger owner alerts, as a potential indication of required maintenance.

## 8 Bibliography

- [1] CRD, “CRD Corporate Climate Action Strategy,” 2016, p. 51. [Online]. Available: [https://www.crd.bc.ca/docs/default-source/crd-document-library/annual-reports/climate/corporateclimateactionstrategy.pdf?sfvrsn=e2372bca\\_4](https://www.crd.bc.ca/docs/default-source/crd-document-library/annual-reports/climate/corporateclimateactionstrategy.pdf?sfvrsn=e2372bca_4).
- [2] NRCan. (Oct. 2013). “Fuel consumption ratings by model year,” [Online]. Available: <https://www.nrcan.gc.ca/energy/efficiency/11938> (visited on 12/21/2018).
- [3] US EPA. “Find and Compare Cars,” [Online]. Available: <http://www.fueleconomy.gov/feg/findacar.shtml> (visited on 10/21/2019).
- [4] H. Huo, Z. Yao, K. He, and X. Yu, “Fuel consumption rates of passenger cars in China: Labels versus real-world,” *Energy Policy*, vol. 39, no. 11, pp. 7130–7135, Nov. 2011, ISSN: 03014215. DOI: [10.1016/j.enpol.2011.08.031](https://doi.org/10.1016/j.enpol.2011.08.031). [Online]. Available: <https://linkinghub.elsevier.com/retrieve/pii/S0301421511006288> (visited on 12/21/2018).
- [5] Mark Huffman. (Jun. 2015). “How accurate is your car’s fuel economy rating?” [Online]. Available: <https://www.consumeraffairs.com/news/how-accurate-is-your-cars-fuel-economy-rating-062615.html> (visited on 12/21/2018).
- [6] “Zero Emission Fleet Initiative Fleet Logging Project - Summary Report Capital Regional District . . . Autumn Umanetz University of Victoria,” p. 46,
- [7] IESVic, “Zero Emissions Fleet Pilot App Feasibility Study,” 2017. [Online]. Available: [https://www.crd.bc.ca/docs/default-source/climate-action-pdf/zefi-feasibilitystudy.pdf?sfvrsn=5a11e0ca\\_2](https://www.crd.bc.ca/docs/default-source/climate-action-pdf/zefi-feasibilitystudy.pdf?sfvrsn=5a11e0ca_2).
- [8] A. Umanetz, “ZEFI Fleet Logging Project - Summary Report,” 2019.

- [9] M. a. L. C. I. Ministry of Energy. “BC-LCFS Requirements - Province of British Columbia,” [Online]. Available:  
<https://www2.gov.bc.ca/gov/content/industry/electricity-alternative-energy/transportation-energies/renewable-low-carbon-fuels/fuel-supplier-compliance-50005> (visited on 02/21/2021).
- [10] BC Hydro, “Greenhouse Gas Intensities,” p. 1, 2016. [Online]. Available:  
<https://www.bchydro.com/content/dam/BCHydro/customer-portal/documents/corporate/environment-sustainability/environmental-reports/ghg-intensities-2004-2014.pdf>.
- [11] BC Government. “Greenhouse Gas Reduction Targets Act,” [Online]. Available:  
[http://www.bclaws.ca/civix/document/id/consol22/consol22/00\\_07042\\_01](http://www.bclaws.ca/civix/document/id/consol22/consol22/00_07042_01)  
(visited on 08/16/2019).
- [12] BC Ministry of Environment, “B.C. Provincial Greenhouse Gas Inventory Report 2007,” 2007. [Online]. Available:  
<https://www2.gov.bc.ca/assets/gov/environment/climate-change/data/provincial-inventory/2007/pir-2007-full-report.pdf>  
(visited on 12/30/2020).
- [13] J. Lesser. “Are electric cars worse for the environment?” The Agenda, [Online]. Available: <https://politi.co/2wHrT9T> (visited on 02/19/2021).
- [14] (Nov. 10, 2017). “Motor Mouth: A few more inconvenient truths about EV CO2 emissions,” Driving, [Online]. Available:  
<https://driving.ca/auto-news/news/motor-mouth-a-few-more-inconvenient-truths-about-ev-co2-emissions> (visited on 02/20/2021).
- [15] M. T. Boykoff and J. M. Boykoff, “Balance as bias: Global warming and the US prestige press,” *Global Environmental Change*, vol. 14, no. 2, pp. 125–136, Jul. 2004, ISSN: 09593780. DOI: [10.1016/j.gloenvcha.2003.10.001](https://doi.org/10.1016/j.gloenvcha.2003.10.001). [Online]. Available:

<https://linkinghub.elsevier.com/retrieve/pii/S0959378003000669>

(visited on 02/20/2021).

- [16] A. Elgowainy, J. Han, J. Ward, F. Joseck, D. Gohlke, A. Lindauer, T. Ramsden, M. Bidy, M. Alexander, S. Barnhart, I. Sutherland, L. Verduzco, and T. J. Wallington, “Current and Future United States Light-Duty Vehicle Pathways: Cradle-to-Grave Lifecycle Greenhouse Gas Emissions and Economic Assessment,” *Environmental Science & Technology*, vol. 52, no. 4, pp. 2392–2399, Feb. 20, 2018, ISSN: 0013-936X, 1520-5851. DOI: [10.1021/acs.est.7b06006](https://doi.org/10.1021/acs.est.7b06006). [Online]. Available: <https://pubs.acs.org/doi/10.1021/acs.est.7b06006> (visited on 02/20/2021).
- [17] NRCan. (Apr. 30, 2018). “2020 Fuel Consumption Guide,” [Online]. Available: <https://www.nrcan.gc.ca/energy-efficiency/energy-efficiency-transportation/fuel-consumption-guide/21002> (visited on 12/30/2020).
- [18] “FuelEconomy.gov - The official U.S. government source for fuel economy information.” [Online]. Available: <http://www.fueleconomy.gov> (visited on 12/30/2020).
- [19] FPInnovations, “Testing and Verification Protocol for Engine and Vehicle After-market Devices,” 2013. [Online]. Available: <https://etvcanada.ca/wp-content/uploads/2013/08/Report-Protocol-EAMDs-Testing-and-Verification.pdf>.
- [20] Transport Canada. (Mar. 10, 2013). “2-cycle testing,” [Online]. Available: <https://web.archive.org/web/20130310085554/http://www.tc.gc.ca/eng/programs/environment-fcp-2cycle-517.htm> (visited on 02/13/2021).
- [21] —, (Oct. 18, 2012). “5-cycle testing,” [Online]. Available: <https://web.archive.org/web/20121018023539/http://www.tc.gc.ca/eng/programs/environment-fcp-5cycle-530.htm> (visited on 02/13/2021).

- [22] NRCan. (Apr. 30, 2018). “Fuel consumption testing,” [Online]. Available: <https://www.nrcan.gc.ca/energy-efficiency/energy-efficiency-transportation/2020-fuel-consumption-guide/understanding-fuel-consumption-r/fuel-consumption-testing/21008> (visited on 12/29/2020).
- [23] —, (Sep. 11, 2018). “EnerGuide label for battery-electric vehicles,” [Online]. Available: <https://www.nrcan.gc.ca/energy/efficiency/energy-efficiency-transportation-and-alternative-fuels/choosing-right-vehicle/tips-buying-fuel-efficient-vehicle/energguide-vehicles/energguide-label-battery-electric-vehicles/21379> (visited on 12/29/2020).
- [24] A. Umanetz, “Classification of fleet micro-trips using kinetic parameters.”
- [25] R. O. Duda, P. E. Hart, and D. G. Stork, *Pattern Classification*, 2nd ed. New York: Wiley, 2001, ISBN: 978-0-471-05669-0.
- [26] (Jul. 9, 2019). “Logistic Regression For Machine Learning and Classification,” Kambria, [Online]. Available: <https://kambria.io/blog/logistic-regression-for-machine-learning/> (visited on 01/01/2021).
- [27] X. Zhang and C. Mi, *Vehicle Power Management: Modeling, Control and Optimization*, ser. Power Systems. London ; New York: Springer Verlag, 2011, ISBN: 978-0-85729-735-8.
- [28] P G Boulter, T J Barlow, S Latham, and I S McCrae, “A reference book of driving cycles for use in the measurement of road vehicle emissions,” Department for Transport, Cleaner Fuels & Vehicles 4.
- [29] EPA. “Dynamometer Drive Schedules | Vehicle and Fuel Emissions Testing | US EPA,” [Online]. Available: <https://www.epa.gov/vehicle-and-fuel-emissions-testing/dynamometer-drive-schedules> (visited on 12/07/2018).

- [30] NREL. “APPENDICES–ADVISOR Documentation,” [Online]. Available: [http://adv-vehicle-sim.sourceforge.net/advisor\\_appendices.html](http://adv-vehicle-sim.sourceforge.net/advisor_appendices.html) (visited on 12/07/2018).
- [31] J. Wu, C. -H. Zhang, and N. -X. Cui, “Fuzzy energy management strategy for a hybrid electric vehicle based on driving cycle recognition,” *International Journal of Automotive Technology*, vol. 13, no. 7, pp. 1159–1167, Dec. 2012, ISSN: 1229-9138, 1976-3832. DOI: [10.1007/s12239-012-0119-z](https://doi.org/10.1007/s12239-012-0119-z). [Online]. Available: <http://link.springer.com/10.1007/s12239-012-0119-z> (visited on 12/08/2018).
- [32] H. Yu, F. Tseng, and R. McGee, “Driving pattern identification for EV range estimation,” in *2012 IEEE International Electric Vehicle Conference*, Greenville, SC, USA: IEEE, Mar. 2012, pp. 1–7, ISBN: 978-1-4673-1561-6. DOI: [10.1109/IEVC.2012.6183207](https://doi.org/10.1109/IEVC.2012.6183207). [Online]. Available: <http://ieeexplore.ieee.org/document/6183207/> (visited on 12/08/2018).
- [33] M. Redelbach, E. D. Özdemir, and H. E. Friedrich, “Optimizing battery sizes of plug-in hybrid and extended range electric vehicles for different user types,” *Energy Policy*, vol. 73, pp. 158–168, Oct. 2014, ISSN: 03014215. DOI: [10.1016/j.enpol.2014.05.052](https://doi.org/10.1016/j.enpol.2014.05.052). [Online]. Available: <https://linkinghub.elsevier.com/retrieve/pii/S030142151400367X> (visited on 12/08/2018).
- [34] R. Smith, S. Shahidinejad, D. Blair, and E. Bibeau, “Characterization of urban commuter driving profiles to optimize battery size in light-duty plug-in electric vehicles,” *Transportation Research Part D: Transport and Environment*, vol. 16, no. 3, pp. 218–224, May 2011, ISSN: 13619209. DOI: [10.1016/j.trd.2010.09.001](https://doi.org/10.1016/j.trd.2010.09.001). [Online]. Available: <https://linkinghub.elsevier.com/retrieve/pii/S1361920910001318> (visited on 12/08/2018).

- [35] L. Evans, R. Herman, and T. N. Lam, "Gasoline Consumption in Urban Traffic," Feb. 1976. DOI: [10.4271/760048](https://doi.org/10.4271/760048). [Online]. Available: <http://papers.sae.org/760048/> (visited on 12/07/2018).
- [36] S. H. Kamble, T. V. Mathew, and G. Sharma, "Development of real-world driving cycle: Case study of Pune, India," *Transportation Research Part D: Transport and Environment*, vol. 14, no. 2, pp. 132–140, Mar. 2009, ISSN: 13619209. DOI: [10.1016/j.trd.2008.11.008](https://doi.org/10.1016/j.trd.2008.11.008). [Online]. Available: <http://linkinghub.elsevier.com/retrieve/pii/S136192090800148X> (visited on 12/07/2018).
- [37] R. Shankar and J. Marco, "Method for estimating the energy consumption of electric vehicles and plug-in hybrid electric vehicles under real-world driving conditions," *IET Intelligent Transport Systems*, vol. 7, no. 1, pp. 138–150, Mar. 2013, ISSN: 1751-956X, 1751-9578. DOI: [10.1049/iet-its.2012.0114](https://doi.org/10.1049/iet-its.2012.0114). [Online]. Available: <https://digital-library.theiet.org/content/journals/10.1049/iet-its.2012.0114> (visited on 12/07/2018).
- [38] H. He, C. Sun, and X. Zhang, "A Method for Identification of Driving Patterns in Hybrid Electric Vehicles Based on a LVQ Neural Network," *Energies*, vol. 5, no. 9, pp. 3363–3380, Sep. 5, 2012, ISSN: 1996-1073. DOI: [10.3390/en5093363](https://doi.org/10.3390/en5093363). [Online]. Available: <http://www.mdpi.com/1996-1073/5/9/3363> (visited on 12/07/2018).
- [39] E. Ericsson, "Independent driving pattern factors and their influence on fuel-use and exhaust emission factors," p. 21, 2001.
- [40] M. Verleysen and D. François, "The Curse of Dimensionality in Data Mining and Time Series Prediction," in *Computational Intelligence and Bioinspired Systems*, vol. 3512, Berlin, Heidelberg: Springer Berlin Heidelberg, 2005, pp. 758–770, ISBN: 978-3-540-26208-4. DOI: [10.1007/11494669\\_93](https://doi.org/10.1007/11494669_93). [Online]. Available: [http://link.springer.com/10.1007/11494669\\_93](http://link.springer.com/10.1007/11494669_93) (visited on 12/11/2018).

- [41] E. Alpaydin, *Introduction to Machine Learning*, 2nd ed, ser. Adaptive Computation and Machine Learning. Cambridge, Mass: MIT Press, 2010, 537 pp., ISBN: 978-0-262-01243-0.
- [42] Falk, Michael, *A First Course on Time Series Analysis*. University of Würzburg, 2012.
- [43] S. L. Sclove, "Time-series segmentation: A model and a method," *Information Sciences*, Institute of Electrical and Electronics Engineers Workshop "Applied Time Series Analysis", vol. 29, no. 1, pp. 7–25, Feb. 1, 1983, ISSN: 0020-0255. DOI: [10.1016/0020-0255\(83\)90007-5](https://doi.org/10.1016/0020-0255(83)90007-5). [Online]. Available: <http://www.sciencedirect.com/science/article/pii/0020025583900075> (visited on 01/03/2021).
- [44] Encyclopedia of Mathematics. "Regression analysis," [Online]. Available: [http://encyclopediaofmath.org/index.php?title=%20Regression\\_analysis&oldid=17714](http://encyclopediaofmath.org/index.php?title=%20Regression_analysis&oldid=17714) (visited on 01/03/2021).
- [45] Karanveer Mohan. "Visualizing K-Means Clustering Webpage," [Online]. Available: <http://stanford.edu/class/ee103/visualizations/kmeans/kmeans.html> (visited on 12/18/2018).
- [46] "Elbow Method — Yellowbrick v1.2 documentation," [Online]. Available: <https://www.scikit-yb.org/en/latest/api/cluster/elbow.html> (visited on 01/01/2021).
- [47] T. Alade. (Dec. 23, 2019). "Tutorial: How to determine the optimal number of clusters for k-means clustering," Medium, [Online]. Available: <https://blog.cambridgespark.com/how-to-determine-the-optimal-number-of-clusters-for-k-means-clustering-14f27070048f> (visited on 01/01/2021).

- [48] “KMeans — scikit-learn 0.24.0 documentation,” [Online]. Available: <https://scikit-learn.org/stable/modules/clustering.html> (visited on 01/01/2021).
- [49] A. H. Maslow, *The Psychology of Science: A Reconnaissance*. Harper & Row, 1966, 200 pp., ISBN: 978-0-8092-6130-7. Google Books: [qitgAAAAMAAJ](#).
- [50] “OBD2 Explained - A Simple Intro (2019),” [Online]. Available: <https://www.csselectronics.com/screen/page/simple-intro-obd2-explained/language/en#OBD2-Intro-Dummies-Basics> (visited on 01/13/2020).
- [51] Texas Instruments. (2002). “Introduction to the Controller Area Network.”
- [52] *SAE On-Board Diagnostics for Light and Medium Duty Vehicles Standards Manual*. SAE International, 2010, ISBN: 978-0-7680-2173-8.
- [53] “The Chemistry of Combustion,” [Online]. Available: <https://www.chem.fsu.edu/chemlab/chm1020c/Lecture%207/01.php> (visited on 01/17/2020).
- [54] N. Goodnight and K. VanGelder, *Automotive Engine Performance*. Jones & Bartlett Learning, Feb. 2019, ISBN: 978-1-284-10206-2. Google Books: [sBmIDwAAQBAJ](#).
- [55] E. R. Jones and R. L. Childers, *Contemporary College Physics*. Addison-Wesley Publishing Company, Jan. 1990, ISBN: 978-0-201-11951-0.
- [56] “Fuels - Higher and Lower Calorific Values,” [Online]. Available: [https://www.engineeringtoolbox.com/fuels-higher-calorific-values-d\\_169.html](https://www.engineeringtoolbox.com/fuels-higher-calorific-values-d_169.html) (visited on 01/17/2020).
- [57] W.-Y. Chang. (Jul. 23, 2013). “The State of Charge Estimating Methods for Battery: A Review,” *ISRN Applied Mathematics*, [Online]. Available: <https://www.hindawi.com/journals/isrn/2013/953792/> (visited on 01/04/2021).

- [58] “2017 Kia Soul EV Specifications,” [Online]. Available:  
<https://www.kiamedia.com/us/en/models/soul-ev/2017/specifications>  
(visited on 01/18/2020).
- [59] “2016 Kia Soul EV Specifications,” [Online]. Available:  
<https://www.kiamedia.com/us/en/models/soul-ev/2016/specifications>  
(visited on 02/02/2020).
- [60] Mitsubishi Motor Corp. (2018). “2018-Mitsubishi-Outlander-PHEV-Brochure,”  
[Online]. Available:  
<https://mcarstatic.cachefly.net/pdf/section/request-a-brochure/2018-Mitsubishi-Outlander-PHEV-Brochure.pdf> (visited on  
02/02/2020).
- [61] “Welcome to LightGBM’s documentation! — LightGBM 3.1.1.99  
documentation,” [Online]. Available:  
<https://lightgbm.readthedocs.io/en/latest/> (visited on 01/18/2021).
- [62] Hastie, Trevor, Tibshirani, Robert, and J. Friedman, *The Elements of Statistical Learning*. Springer, 2017.
- [63] “Jamesajeeth/Data-Science,” GitHub, [Online]. Available:  
<https://github.com/jamesajeeth/Data-Science> (visited on 02/19/2021).
- [64] “Gradient Boosting in Python from Scratch | by Carl Dawson | Towards Data  
Science,” [Online]. Available: <https://towardsdatascience.com/gradient-boosting-in-python-from-scratch-4a3d9077367> (visited on 02/19/2021).
- [65] “Parameters Tuning — LightGBM 3.1.1.99 documentation,” [Online]. Available:  
<https://lightgbm.readthedocs.io/en/latest/Parameters-Tuning.html>  
(visited on 02/08/2021).
- [66] G. Ke, Q. Meng, T. Finley, T. Wang, W. Chen, W. Ma, Q. Ye, and T.-Y. Liu,  
“LightGBM: A Highly Efficient Gradient Boosting Decision Tree,” p. 9,

- [67] “Scikit-optimize: Sequential model-based optimization in Python — scikit-optimize 0.8.1 documentation,” [Online]. Available: <https://scikit-optimize.github.io/stable/> (visited on 02/01/2021).
- [68] fernando, *Fmf/n/BayesianOptimization*, Feb. 21, 2021. [Online]. Available: <https://github.com/fmf/n/BayesianOptimization> (visited on 02/21/2021).
- [69] “Tuning Hyperparameters Under 10 Minutes (LGBM),” [Online]. Available: <https://kaggle.com/somang1418/tuning-hyperparameters-under-10-minutes-lgbm> (visited on 02/01/2021).
- [70] NRCan. “Fuel consumption ratings search tool,” [Online]. Available: <https://fcr-ccc.nrcan-rncan.gc.ca/en> (visited on 02/14/2021).
- [71] S. Lundberg and S.-I. Lee. (Nov. 24, 2017). “A Unified Approach to Interpreting Model Predictions.” arXiv: [1705.07874](https://arxiv.org/abs/1705.07874) [cs, stat], [Online]. Available: <http://arxiv.org/abs/1705.07874> (visited on 02/21/2021).
- [72] S. Mazzanti. (Apr. 26, 2020). “SHAP explained the way I wish someone explained it to me,” Medium, [Online]. Available: <https://towardsdatascience.com/shap-explained-the-way-i-wish-someone-explained-it-to-me-ab81cc69ef30> (visited on 02/21/2021).
- [73] S. Lundberg, *Slundberg/shap*, Jan. 24, 2021. [Online]. Available: <https://github.com/slundberg/shap> (visited on 01/24/2021).
- [74] BC Ministry of Environment, “2016 B.C. BEST PRACTICES METHODOLOGY FOR QUANTIFYING GREENHOUSE GAS EMISSIONS,” 2016. DOI: [10.1007/s12273-013-0159-y](https://doi.org/10.1007/s12273-013-0159-y).
- [75] C. Atiyeh. (Dec. 4, 2019). “Everything You Need to Know about the VW Diesel-Emissions Scandal,” Car and Driver, [Online]. Available: <https://www.caranddriver.com/news/a15339250/everything-you-need-to-know-about-the-vw-diesel-emissions-scandal> (visited on 01/02/2021).
- [76] Bullfrog Power, *Canadian Emission Factors for Grid Electricity*, 2015.

- [77] I. Khan, M. W. Jack, and J. Stephenson, "Use of time-varying carbon intensity estimation to evaluate GHG emission reduction opportunities in electricity sector," in *2017 IEEE Conference on Technologies for Sustainability (SusTech)*, Phoenix, AZ: IEEE, Nov. 2017, pp. 1–2, ISBN: 978-1-5386-0452-6. DOI: [10.1109/SusTech.2017.8333479](https://doi.org/10.1109/SusTech.2017.8333479). [Online]. Available: <https://ieeexplore.ieee.org/document/8333479/> (visited on 02/15/2021).
- [78] P. S. Maybeck, *Stochastic Models, Estimation and Control*, ser. Mathematics in Science and Engineering v. 141. New York: Academic Press, 1979, 3 pp., ISBN: 978-0-12-480701-3.
- [79] Mueller, M., *Information Retrieval for Music and Motion*. Springer, 2007, ISBN: 978-3-540-74047-6. [Online]. Available: <http://www.springer.com/978-3-540-74047-6>.
- [80] D. Li, T. F. Bissyandé, J. Klein, and Y. L. Traon, "Time Series Classification with Discrete Wavelet Transformed Data: Insights from an Empirical Study," presented at the The 28th International Conference on Software Engineering and Knowledge Engineering, Jul. 1, 2016, pp. 273–278. DOI: [10.18293/SEKE2016-067](https://doi.org/10.18293/SEKE2016-067). [Online]. Available: [http://ksiresearchorg.ipage.com/seke/seke16paper/seke16paper\\_67.pdf](http://ksiresearchorg.ipage.com/seke/seke16paper/seke16paper_67.pdf) (visited on 12/07/2018).
- [81] NRCan. "High Resolution Digital Elevation Model (HRDEM) - CanElevation Series - Open Government Portal," [Online]. Available: <https://open.canada.ca/data/en/dataset/957782bf-847c-4644-a757-e383c0057995> (visited on 01/01/2021).
- [82] Freematics.com. "Freematics ONE+ Model B spec sheet," [Online]. Available: <https://freematics.com/pages/products/freematics-one-plus-model-b/> (visited on 01/01/2021).
- [83] —, "Freematics Packed Data Format," [Online]. Available: <https://freematics.com/pages/hub/freematics-data-logging-format/> (visited on 01/01/2021).

- [84] Ministry of Energy, Mines and Petroleum Resources, *Carbon Intensity Records under the Renewable and Low Carbon Fuel Requirements Regulation*.
- [85] BC Hydro, “Greenhouse Gas Intensities 2007, 2011-2015,” p. 1,
- [86] J. I. Levene, M. K. Mann, R. M. Margolis, and A. Milbrandt, “An analysis of hydrogen production from renewable electricity sources,” *Solar Energy*, vol. 81, no. 6, pp. 773–780, Jun. 2007, ISSN: 0038092X. DOI: [10.1016/j.solener.2006.10.005](https://doi.org/10.1016/j.solener.2006.10.005). [Online]. Available: <https://linkinghub.elsevier.com/retrieve/pii/S0038092X06002635> (visited on 02/21/2021).
- [87] A. Umanetz, “Well-to-Wheel GHG Intensity for Vehicular Hydrogen Fuel in British Columbia,” University of Victoria, (Unpublished), 2018.
- [88] B. James, “Current Forecourt Hydrogen Production from Natural Gas (1,500 kg per day) version 3.101,” NREL, 2012.
- [89] O. Schmidt, A. Gambhir, I. Staffell, A. Hawkes, J. Nelson, and S. Few, “Future cost and performance of water electrolysis: An expert elicitation study,” *International Journal of Hydrogen Energy*, vol. 42, no. 52, pp. 30 470–30 492, Dec. 2017, ISSN: 03603199. DOI: [10.1016/j.ijhydene.2017.10.045](https://doi.org/10.1016/j.ijhydene.2017.10.045). [Online]. Available: <https://linkinghub.elsevier.com/retrieve/pii/S0360319917339435> (visited on 02/21/2021).

## A Logger features

Table 14: CRD FleetCarma logger features

Feature	Unit	Comment
Absolute Load	[%]	
Air Conditioning Power	[W]	
Altitude	[m]	GPS
C2 Input Voltage	[V]	
Charge Latitude	[deg]	
Charge Longitude	[deg]	
Engine RPM	[RPM]	
GpsAlt	(m)	
GpsLat	(deg)	
GpsLon	(deg)	
HDOP		
HV Battery Current	[A]	
HV Battery SOC	[%]	
HV Battery Voltage	[V]	
Heater Power	[W]	
Is Charging	[bool]	
Is Driving	[bool]	
Latitude	[deg]	GPS
LoggerName		
Longitude	[deg]	GPS
MAF	[g/sec]	
NumberOfSatellites	GPS	
OAT	[degC]	
Pck		
Signal #131		Speed
Start Time	(UTC)	
Time	(UTC)	
Timestamp	(ms)	
Vehicle Speed	[km/h]	
Vin		

## B Embodied energy and Fuel Intensity

This is a discussion of assumptions and sources needed to convert life-cycle analysis (LCA) figures by Elgowainy et al [16] to apply study-contemporaneous and forecasted fuel intensities for BC. Detailed column calculations are shown for 2018 in table 15 and for 2030 in table 16.

### B.0.1 Vehicle assumptions

Elgowainy's (reasonable) PHEV efficiency figure was not supported; to properly apportion emissions to gasoline and BC grid electricity, Elgowainy's figure was decomposed and found to imply an operational regime of 27.1% in BEV mode for 2018, and at 28.0% BEV mode in 2030.

In order to give a fair apples-to-apples comparison, the BEV90 was given the full lifetime travel distance of 286,000 km, differing from Elgowainy's treatment, which amortized the vehicle' manufacturing emissions over a much shorter lifetime travel distance.

### B.0.2 Legend for LCA tables

Legend for tables 15 and 16:

- MPGGE: miles per gallon, gasoline equivalent, taken directly from Elgowainy
- Le/100km: MPGGE directly converted to metric Gasoline-equivalent litres per 100km
- Fuel Intensity: assumptions and sources are discussed in the remainder of this section
- Tailpipe: total lifetime tailpipe emissions, at Elgowainy's assumption of a 15-year vehicle life of 286,000 km (178,000 miles)
- Vehicle: total vehicle manufacturing and decommissioning emissions
- Lifetime: sum of Tailpipe and Vehicle fields
- Amortized: Lifetime emissions, divided by lifetime travel distance.

Table 15: Calculations to apply BC intensities to 2018 vehicle LCA

		ICEV	HEV	PHEV35	FCEV	BEV90
Efficiency	(MPGGE)	26.2	36.5	53.7	54.1	100
	(Le/100km)	8.98	6.44	4.38	4.35	2.34
	(MJ/km)	3.04	2.18	1.48	1.47	0.793
Fuel Intensity	(gCO <sub>2</sub> e/MJ)	88.1	88.1	64.9	5.	2.5
Emission	(gCO <sub>2</sub> e/km)	268	192	96.3	7.37	1.98
Tailpipe	(tCO <sub>2</sub> e)	76.8	55.1	27.6	2.11	0.568
Vehicle	(tCO <sub>2</sub> e)	7.78	8.2	9.4	11.7	7.9
Lifetime	(tCO <sub>2</sub> e)	84.6	63.3	37	13.8	8.47
Amortized	(gCo <sub>2</sub> e/km)	295	221	129	48.2	29.6
Battery-mode	(fraction)	0	0	0.271	0	1

Table 16: Calculations to apply BC intensities to 2030 vehicle LCA

		ICEV	HEV	PHEV35	FCEV	BEV90
Efficiency	(MPGge)	34.5	53.5	72	72	120
	(Le/100km)	6.82	4.4	3.27	3.27	1.97
	(MJ/km)	2.31	1.49	1.11	1.11	0.667
Fuel Intensity	(gCO <sub>2</sub> e/MJ)	70.5	70.5	51.1	1.18	1.11
Emission	(gCO <sub>2</sub> e/km)	163	105	56.5	1.31	0.74
Tailpipe	(tCO <sub>2</sub> e)	46.6	30.1	16.2	0.375	0.212
Vehicle	(tCO <sub>2</sub> e)	6.9	7.1	7.6	9.5	6.4
Lifetime	(tCO <sub>2</sub> e)	53.5	37.2	23.8	9.88	6.61
Amortized	(gCo <sub>2</sub> e/km)	187	130	83.1	34.5	23.1
Battery-mode	(fraction)	0	0	0.28	0	1

- Battery-mode: Fraction of time that PHEV is assumed to be operating from grid power

### B.0.3 Intensity assumptions - 2018

**Gasoline:** The MOE published a 2018 intensity of 88.1 g CO<sub>2</sub>e/MJ [84].

**BC grid power:** BC Hydro’s published intensity of 2.50 g CO<sub>2</sub>e/MJ for grid power is the average of internal generation, and that purchased from independent power producers [85].

**Hydrogen fuel:** For the small volumes required by the current low adoption rates for FCEVs, it is reasonable to assume a carbon intensity for H<sub>2</sub> gas of 5.0 g CO<sub>2</sub>e/MJ. This figure is based on the energy requirements for small-scale electrolysis [86] at BC Hydro’s grid power intensity, and short-range transportation in high-pressure tube trailers [87].

At higher volumes, it would in the short term likely be necessary to import hydrogen

produced by steam-methane reformation, at a probable intensity of 85.3 g CO<sub>2e</sub>/MJ [88].

#### **B.0.4 Intensity assumptions - 2030**

The following forecasts were used for 2030 fuel carbon intensities.

**Gasoline:** 70.51 g CO<sub>2e</sub>/MJ as required under the BC Renewable & Low Carbon Fuel Requirements Regulation [9].

**BC Hydro grid electricity:** 1.11 g CO<sub>2e</sub>/MJ. In the absence of any public goal or regulatory target, it seems reasonable to expect to use the intensity of BC Hydro's directly owned facilities; on the assumption that there will be pressure on external independent power producers to find low-carbon power sources, or require them to purchase offsets [85]. This will vary depending on the level of import/export trade, any changes in the associated carbon accounting practices, and the amortized emission associated with the Site C hydroelectric project.

**Hydrogen fuel:** Schmidt et al [89] suggest that H<sub>2</sub> electrolysis efficiency will not improve significantly. However, the same work states that a solid-oxide electrolyser can take much of its input energy in the form of heat, and can deliver electrical efficiencies in excess of 100%. The assumed 2030 intensity of 1.18 g CO<sub>2e</sub>/MJ for H<sub>2</sub> gas [87] is a best-case assumption, predicated on the existence of an SOEC plant with a source of zero-impact industrial heat, and fully powered by electricity at BC Hydro's internal grid power intensity.